Gastroenterology 2018;155:514–528

Optogenetic Induction of Colonic Motility in Mice

Timothy J. Hibberd,[1,*] **Jing Feng**,[2,*] Jialie Luo,[2] Pu Yang,[2] Vijay K. Samineni,[3] Robert W. Gereau IV,[3] Nigel Kelley,[4] Hongzhen Hu,[2,§] and Nick J. Spencer[1,§]

[1]College of Medicine and Public Health and Centre for Neuroscience, Flinders University, Adelaide, Australia; [2]Department of Anesthesiology, The Center for the Study of Itch, Washington University School of Medicine, St Louis, Missouri; [3]Washington University Pain Center, Department of Anesthesiology, Washington University School of Medicine, St Louis, Missouri; and [4]SA Biomedical Engineering, SA Health, Government of South Australia, Adelaide, Australia

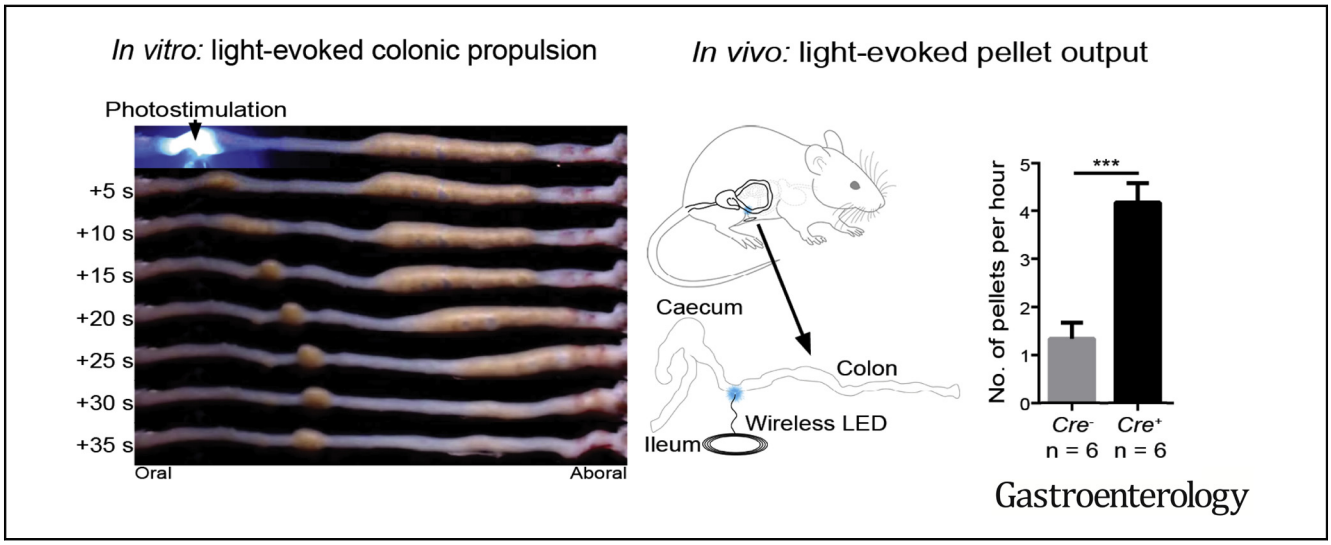

BACKGROUND & AIMS: Strategies are needed to increase gastrointestinal transit without systemic pharmacologic agents. We investigated whether optogenetics, focal application of light to control enteric nervous system excitability, could be used to evoke propagating contractions and increase colonic transit in mice. **METHODS:** We generated transgenic mice with Cre-mediated expression of light-sensitive channelrhodopsin-2 (ChR2) in calretinin neurons (CAL-ChR2 *Cre*+ mice); *Cre*– littermates served as controls. Colonic myenteric neurons were analyzed by immunohistochemistry, patch-clamp, and calcium imaging studies. Motility was assessed by mechanical, electrophysiological, and video recording in vitro and by fecal output in vivo. **RESULTS:** In isolated colons, focal light stimulation of calretinin enteric neurons evoked classic polarized motor reflexes (50/58 stimulations), followed by premature anterograde propagating contractions (39/58 stimulations). Light stimulation could evoke motility from sites along the entire colon. These effects were prevented by neural blockade with tetrodotoxin (n = 2), and did not occur in control mice (n = 5). Light stimulation of proximal colon increased the proportion of natural fecal pellets expelled over 15 minutes in vitro (75% ± 17% vs 32% ± 8% for controls) ($P < .05$). In vivo, activation of wireless light-emitting diodes implanted onto the colon wall significantly increased hourly fecal pellet output in conscious, freely moving mice (4.2 ± 0.4 vs 1.3 ± 0.3 in controls) ($P < .001$). **CONCLUSIONS:** In studies of mice, we found that focal activation of a subset of enteric neurons can increase motility of the entire colon in vitro, and fecal output in vivo. Optogenetic control of enteric neurons might therefore be used to modify gut motility.

Keywords: Peristalsis; Gut Motility; Colonic Migrating Motor Complex; Myoelectric Complex.

Compared with all other internal organs, the gastrointestinal tract is unique in that it possesses an independent nervous system, known as the enteric nervous system (ENS).[1,2] Comprising similar numbers of neurons as the spinal cord, the ENS has intrinsic sensory neurons

*Authors share co-first authorship; §Authors share co-senior authorship.

Abbreviations used in this paper: **CAL, calretinin; ChAT, choline acetyltransferase; CNS, central nervous system; ENS, enteric nervous system; NOS, nitric oxide synthase; ChR2, channelrhodopsin-2; Cre-recombinase, causes recombination; eYFP, enhanced yellow fluorescent protein; PBS, phosphate-buffered saline; TTX, tetrodotoxin.**

Most current article

0016-5085/$36.00
https://doi.org/10.1053/j.gastro.2018.05.029

WHAT YOU NEED TO KNOW

BACKGROUND AND CONTEXT

Strategies are needed to increase GI transit without systemic pharmacologic agents. Optogenetic control of the enteric nervous system could be used to control GI motility and transit using light.

NEW FINDINGS

Light-activation of colonic calretinin neurons evoked classic polarized motor reflexes and propulsive contractions, in vitro. Light-stimulation in conscious, freely behaving mice using wireless microLED implants increased pellet expulsion, in vivo.

LIMITATIONS

The occurrence of calretinin in multiple subclasses of enteric neurons limits the mechanistic insight of the study.

IMPACT

The study provides proof of principle that optical control of enteric neurons can be used to modify GI motility.

within the gut wall, in addition to populations of interneurons and excitatory and inhibitory motor neurons. Enteric neurons coordinate complex behaviors fully autonomous of the central nervous system (CNS). Perhaps the best demonstration of this, is that isolated segments of bowel are capable of generating propulsive gut motility without CNS input.[3] ENS activity is essential for the coordinated release of excitatory neurotransmitters onto smooth muscle, facilitating contraction of smooth muscle and propulsion of ingested content. Optogenetics has been well established in the CNS, but comparatively less so in the peripheral nervous system. The possibility of using focal application of light to control ENS excitability and improve transit of contents without using agonists that act in multiple organ systems with off-target effects, is particularly attractive.

Calretinin is a calcium-binding protein encoded by the gene calbindin 2. Calretinin is expressed by a subset of myenteric neurons involved in gut motility. These include cholinergic motor neurons, interneurons, and putative sensory neurons.[4,5] Propagating contractions of the murine large intestine has a neural origin (neurogenic).[6] Intrinsic primary sensory neurons, which express calretinin, may initiate propagating neurogenic contractions, also referred to as "colonic migrating motor complexes", or CMMCs.[7] We hypothesized that expression of the light-sensitive cation channel, channelrhodopsin2 in calretinin neurons would enable control of colonic neurogenic contractions.

In this study, we generated mice expressing channelrhodopsin2 (ChR2) and enhanced yellow fluorescent reporter protein (eYFP), in cells expressing calretinin (*CAL-ChR2*$^{Cre+}$; see Methods section). Focal light-activation of calretinin enteric neurons evoked polarized motor reflexes and propulsive neurogenic contractions in vitro, leading to significantly increased expulsion of natural fecal pellets both in vitro and in vivo. Parts of this study have been published in abstract form.[8]

Methods

Animals

Calb2-IRES-Cre (B6(Cg)-*Calb2*$^{tm1(cre)Zjh}$/J) and Rosa-CAG-LSL-ChR2(H134R)-eYFP-WPRE (Ai32,[9] B6.Cg-*Gt(ROSA)26Sor*$^{tm32(CAG-COP4*H134R/EYFP)Hze}$/J) mice were obtained from Jackson Laboratories (Bar Harbor, ME). Mice expressing Cre-recombinase (causes recombination) were crossbred with Ai32 mice (Figure 1*C*). Resulting *CAL-ChR2*$^{Cre+}$ progeny expressed the ChR2(H134R)-eYFP fusion gene in cells expressing the CALB2 gene product, CAL. All mice were housed under a 12-hour light/dark cycle with food and water provided ad libitum. Experiments were done by observers blind to the treatments or genotypes of animals. All mice used for behavior tests were genotyped and allocated to experimental groups or control groups. *Cre*$^{-}$ littermates were used as controls in all experiments. Strictly matched mice (gender, age) were used at 8 to 12 weeks old for all the experiments. Animal studies are reported in compliance with the ARRIVE guidelines. All experiments were performed in accordance with the guidelines of the National Institutes of Health and the International Association for the Study of Pain, and were approved by the Animal Studies Committee at Washington University School of Medicine.

Tissue Preparation

Mice were killed by cervical dislocation. The abdomen was immediately opened and the entire colon from caecum to terminal rectum was removed. In all experiments except the imaging of natural pellet expulsion, the full length of colon was placed in a Petri dish filled with carbogen-gassed (95% O_2 / 5% CO_2) Krebs solution (25–30°C; in 10^{-3} M concentrations: NaCl 118; KCl 4.7; NaH_2PO_4 1; $NaHCO_3$ 25; $MgCl_2$ 1.2; D-Glucose 11; $CaCl_2$ 2.5). Residual pellets were gently flushed from the colon using Krebs solution and mesentery was removed. For recording natural pellet expulsion in vitro, the terminal rectum was occluded by tying off with fine suture thread before the colon was removed from the animal.

Immunohistochemistry

For immunohistochemical analysis, the colon was pinned into a Krebs-filled, Slygard-lined Petri dish. Preparations were made into a flat sheet by cutting longitudinally along the mesenteric attachment. Preparations were fixed under maximal stretch in modified Zamboni fixative (2% formaldehyde, 0.2% saturated picric acid in 0.1M phosphate buffer, pH 7.0) for approximately 24 hours at 4°C. Tissue was cleared with 3 washes of 100% dimethyl sulfoxide, and stored in phosphate-buffered saline (PBS) at 4°C. To improve visualization of myenteric ganglia, the mucosa, submucosa, and longitudinal muscle layers were removed by sharp dissection.

Preparations of circular muscle and myenteric plexus were incubated with antisera to calretinin (1:500, AB5054; Millipore, Bedford, MA), choline acetyl-transferase (1:50, AB144P; Millipore) or nitric oxide synthase (NOS) (1:300, AB1529; Millipore) at room temperature for 2 days. Preparations were then rinsed 3 times using PBS and incubated with appropriate secondary antisera (1:300, donkey anti-rabbit, catalog no. 711165152; donkey anti-goat, catalog no. A11055, Invitrogen, Carlsbad, CA, or donkey anti-sheep, catalog no. 713095147,

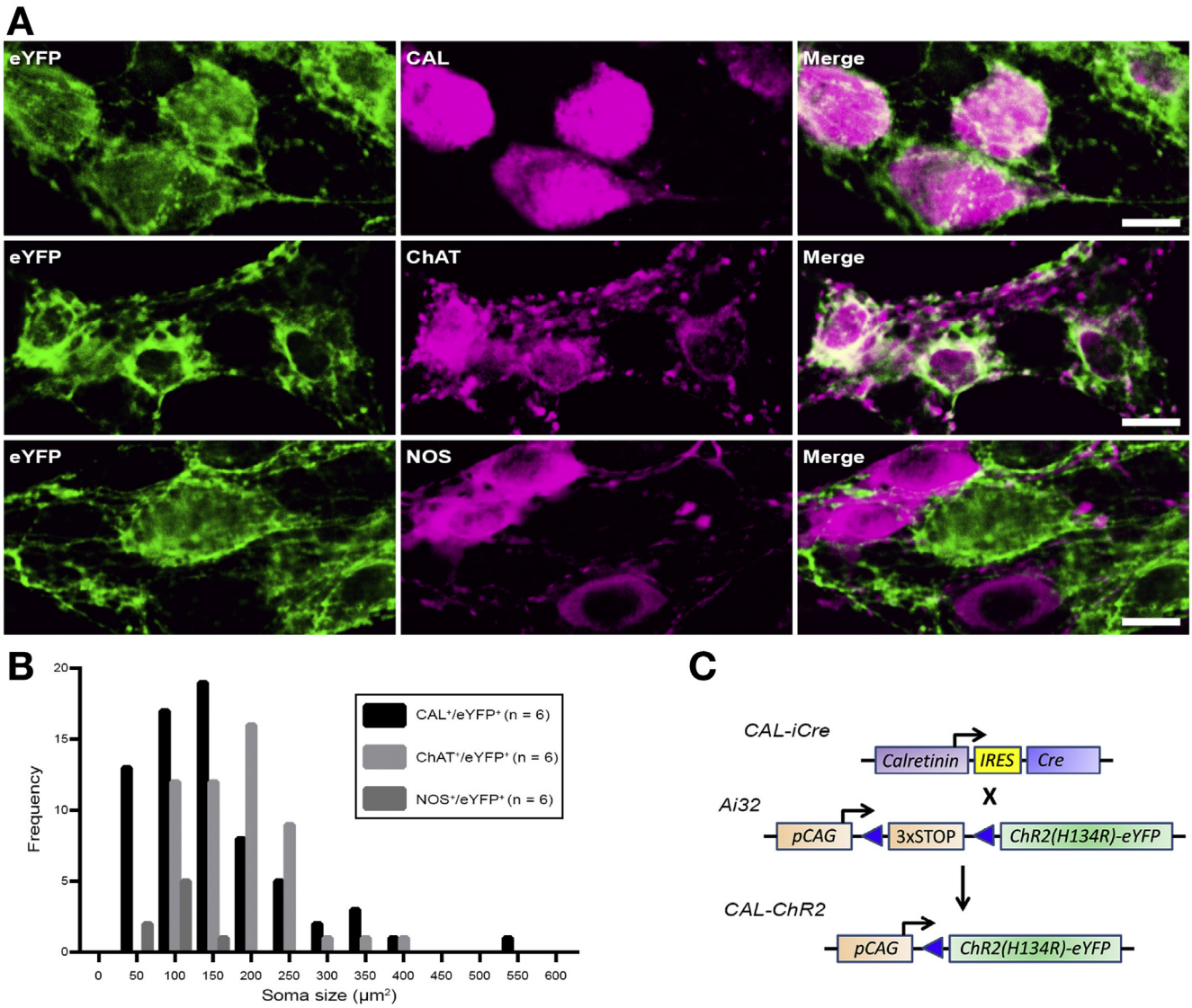

Figure 1. Neurochemical and morphological characterization of eYFP^{+} myenteric neurons. (*A*) Matched micrographs in rows showing excitatory colonic myenteric neurons immunoreactive for CAL and ChAT and inhibitory neurons for NOS, which are also immunoreactive for eYFP. Cytoplasmic eYFP fluorescence occurred in numerous myenteric nerve cell bodies and neurites. Almost all eYFP-fluorescent nerve cell bodies contained immunohistochemically detectable CAL (top row; 97% ± 3%, n = 6), and most contained ChAT (middle row; 79% ± 7%, n = 5). Fewer eYFP neurons also contained NOS immunoreactivity (lower row; 12% ± 5%, n = 7). (*B*) Frequency histogram showing soma sizes among eYFP-fluorescent neurons that contained CAL, ChAT, and NOS immunoreactive content. (*C*) Gene construct diagram of the generation of calretinin-channelrhodopsin (*CAL-ChR2*) mice.

Jackson ImmunoResearch Laboratories, Inc, West Grove, PA) for 4 hours at room temperature. After a final rinse with PBS, preparations were equilibrated with 50%, 70%, and 100% carbonate-buffered glycerol, and mounted in 100% carbonate-buffered glycerol (pH 8.6). All antibodies were diluted in 0.1M PBS (0.3 M NaCl) containing 0.1% sodium azide. Controls were performed by omitting primary antibodies from the procedure and ensuring that the associated secondary antisera no longer labeled structures in the tissue. Colocalization of eYFP fluorescence and CAL, choline acetyltransferase (ChAT), and NOS immunoreactivity was quantified in myenteric ganglia from segments of proximal, middle, and distal colon.

Isolation and Short-Term Culture of Mouse Colonic Myenteric Neurons

The colon was placed in ice-cold Hank's balanced salt solution[10] containing, in 10^{-3}M concentrations: NaCl 137.9, KCl 5.3, $NaHCO_3$ 4.2, $CaCl_2$ 1.3, $MgCl_2$, 0.5, KH_2PO_4 0.4, $MgSO_4$ 0.4 Na_2HPO_4 0.3, and D-Glucose 5.6. Neurons were acutely dissociated and maintained as described in detail elsewhere.[11] Briefly, a strip of longitudinal muscle with myenteric plexus attached was removed from underlying circular muscle of the colon. Longitudinal muscle-myenteric plexus preparations were digested using collagenase type 2 and trypsin. Single cells were collected and plated on coverslips. Following 24 to 48 hours in

culture, neurons were used for calcium imaging and electrophysiological recordings.

Live-Cell Ca^{2+} Imaging

Cultured myenteric neurons were loaded with calcium-sensitive indicators by applying 4 μM Fura-2 AM (Life Technologies, Carlsbad, CA) into the culture medium at 37°C for 60 minutes.[12] Cells were then washed 3 times and incubated in Hank's balanced salt solution at room temperature for 30 minutes before use.[13] CAL^+ neurons were identified by an inverted microscope with a filter set for eYFP visualization. Fluorescence at 340 nm and 380 nm excitation wavelengths was recorded on an inverted Nikon Ti-E microscope equipped with 340-, 360-, and 380-nm excitation filter wheels using NIS-Elements imaging software (Nikon Instruments Inc., Melville, NY). Fura-2 ratios (F340/F380) reflecting changes in intracellular [Ca^{2+}] were monitored and recorded. Values were obtained from 100 to 250 cells in time-lapse images from each coverslip. The threshold of activation was defined as 3 standard deviations above the average (~20% above the baseline[14]).

Patch-Clamp Electrophysiology

Whole-cell patch-clamp recordings were performed at room temperature (22°C–24°C) using an Axon 700B amplifier (Molecular Devices, Sunnyvale, CA) on the stage of an inverted phase-contrast microscope equipped with a filter set for eYFP visualization (Nikon Instruments Inc.).[15] Pipettes pulled from borosilicate glass (BF 150-86-10; Sutter Instrument, Novato, CA) with a Sutter P-1000 pipette puller had resistances of 2 to 4 MΩ for whole-cell patch-clamp recordings when filled with pipette solution containing, in 10^{-3} M concentrations, the following: KCl 140, $MgCl_2$ 1, Mg-ATP 3, EGTA 1, sucrose 10, and HEPES 10 with pH 7.3 and 315 mOsm/L osmolarity. Cells were continuously perfused with standard extracellular solution containing, in 10^{-3} M concentrations, the following: NaCl 140, KCl 5, EGTA 0.5, $MgCl_2$ 1, $CaCl_2$ 2, D-Glucose 10, and HEPES 10 (pH 7.4 and 340 mOsm/L osmolarity). Whole-cell membrane currents were recorded using gap-free recording at holding potential of −60 mV. Data were acquired using Clampex 10.4 software (Molecular Devices, Novato, CA). Currents were filtered at 2 kHz and digitized at 10 kHz. Data were analyzed and plotted using Clampfit 10 (Molecular Devices).

Combined Mechanical and Extracellular Electrophysiological Recordings

Full-length colon preparations were placed in an organ bath (volume ~50 mL). The organ bath was continuously superfused at a rate of approximately 4.6 mL.min^{-1} (36°C). A stainless-steel tube (diameter 1 mm) placed through the lumen was fitted at each end into L-shaped barbed plastic connectors that were fixed to the organ bath base. The oral and anal ends of colon were tied over the barbed connectors with a fine suture thread. Stainless-steel hooks (500 μm diameter) were threaded through the gut wall of the proximal, middle, and distal colon. A fine suture thread connected each hook to an isometric force transducer (MLT050/D; ADInstruments, Bella Vista, NSW, Australia) and set to a basal tension of 0.5 g to record mechanical activity. Activity was recorded at 1 kHz (PowerLab 16/35, LabChart 8; ADInstruments).

During mechanical recordings, conventional extracellular recordings[16] were made from the colonic serosa between the middle and distal force transducers (see Supplementary Figure 1 for a schematic diagram). Two Krebs-filled suction electrodes (AgCl, 250 μm) with heat-polished glass capillary tips were used (0.86 mm internal diameter, 1.5 mm outer diameter; catalog no. 30-0053; Harvard Apparatus, Holliston, MA). Flexible Silastic tubing (Dow Corning Corporation, Midland, MI) connected the glass tip to the AgCl electrode. Signals were amplified (ISO80; WPI, Sarasota, FL) and recorded at 1 kHz (PowerLab; ADInstruments). The signals recorded were in principle assumed to represent extracellular recording of changes in polarity along the surface of the smooth muscle cells.

Natural Pellet Expulsion and Spatio-Temporal Mapping, In Vitro

The full length of colon containing natural pellets was placed into a Krebs-filled, Sylgard-lined organ bath (Sylgard 184; Dow Corning Corporation). Preparations were held in place without obstructing the passage of pellets using etymological pins[17] (500 μm diameter). The suture was then cut free and expulsion of natural pellets was observed over 30 minutes. Light stimulation (20-ms pulse width, 5 Hz, 20-second train duration) was applied to the mid-proximal colon at 3-minute intervals for 30 minutes. Gut movements were recorded by video camera above the organ bath (Carl Zeiss Tessar C920; 800 × 600-pixel resolution, 15 fps; Logitech International SA, Lausanne, Switzerland). Video records were transformed into maps of circumferential gut diameter (diameter maps) using the spatio-temporal mapping technique described by Hennig et al.[18]

Light Stimulation Apparatus

Blue light was generated for in vitro studies with a diode-pumped solid-state laser system (473 nmλ, 50 mW, Model number: CL473-050-O; CrystaLaser LC, Reno, NV). Trains of light pulses (20-ms pulse width, 5 Hz, 20-second train duration) were delivered focally via glass fiberoptic (200 μm diameter; area of direct illumination: 0.0987 mm^2). For experiments in vivo, wireless subdermal optoelectronic implants were used (Neurolux, Champaign, IL; Figure 7*E*). These devices were characterized in detail previously.[19] Briefly, the main body of the device comprised an approximately 9.8-mm diameter circular conductive receiver coil (see photo, Figure 7*E*) and surface-mounted capacitor and rectifier. A malleable interconnect trace carried metal lines for power transmission from the coil to a μLED on an injectable needle (LED dimensions in μm: 270 × 220 × 50; area of direct illumination: 0.0594 mm^2). Power was transferred to the coil by magnetic coupling to a transmission antenna that encircled each recording chamber and emitted electromagnetic waves at radio frequency (13.56 MHz). The μLED emitted 470 nmλ photons. In addition, a μLED (C470DA2432; Cree Inc., Research Triangle Park, NC) driven by a variable power supply was used to characterize the effect of light power density on the efficacy of stimulating colonic motility in vitro (Supplementary Figure 4). Pulse timing was controlled by a Powerlab via an ILD1 optoisolator. The area of light emission was 240 μm × 320 μm (0.0768 mm^2). Light power density across a range of currents

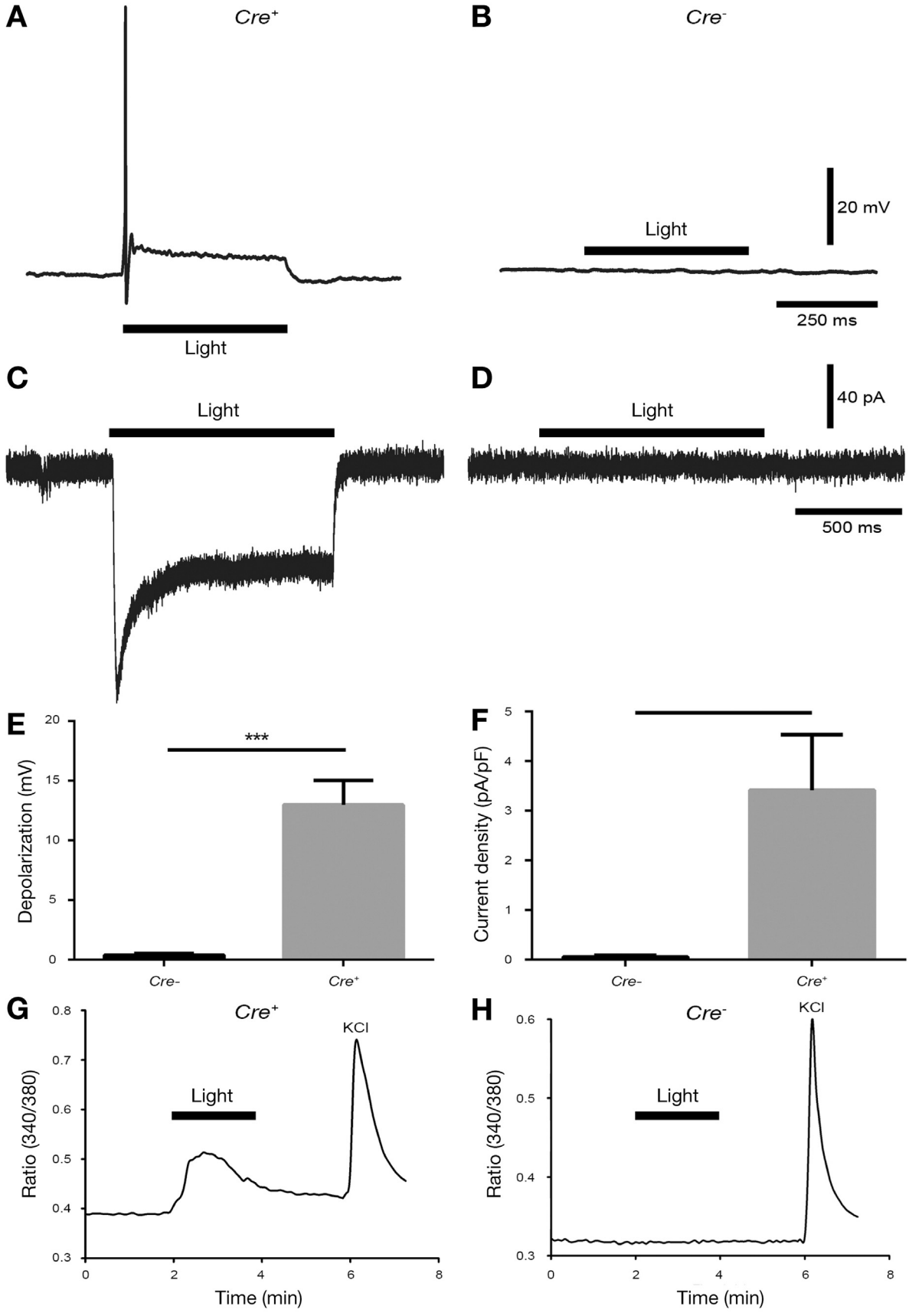
A
Cre+
Light
B
Cre-
20 mV
Light
250 ms
C
Light
D
Light
40 pA
500 ms
E
***
Depolarization (mV)
Cre-
Cre+
F
Current density (pA/pF)
Cre-
Cre+
G
Cre+
KCl
Light
Ratio (340/380)
Time (min)
H
Cre-
KCl
Light
Ratio (340/380)
Time (min)

was measured 5 mm from the LED using a standard photodiode power sensor (S120C; Thorlabs, Newton, NJ) and a power meter (PM100USB; Thorlabs).

Stimulation of Pellet Output, In Vivo

Mice were anesthetized in an induction chamber (4% isoflurane) and maintained at 1% to 2% isoflurane. The body of the wireless optoelectronic implant was inserted between the skin and peritoneum. The implant needle, containing the μLED, was inserted through an incision ($\sim$2 mm) in the peritoneum. The μLED apposed the proximal colon, just distal to the cecocolonic junction.

Mice were acclimated in custom recording chambers for at least 7 days before surgery. Following implantation, mice were supplied soft gel food (DietGel 76A; ClearH2O, Westbrook, ME) and placed on a warm plate during recovery. Mice were returned to recording chambers 2 to 3 days after implantation and pellet output was recorded for 2 hours: 1 hour control and 1 hour with light stimulation (2 Hz, 200-ms pulse width). Recordings were conducted on *Cre*$^{+}$ and *Cre*$^{-}$ (control) mice simultaneously in separate, parallel chambers. Pellets were collected and counted at the end of each hour recording period.

Statistics and Analysis

Spatio-temporal maps were generated from video recordings using computer script for MATLAB software (MathWorks Incorporated, Natick, MA). Script was written in-house at Flinders University (Lukasz Wiklendt, Flinders University). Diameter maps are generated by measuring gut diameter at each point along the preparation in every video frame and converting diameters into grayscale pixels to create a spatio-temporal map of diameter changes. Regions of minimal diameter (contraction) are represented as white pixels, whereas maximal diameter (distension) are represented by black pixels. This method was adapted from what was described in detail elsewhere.[18] Diameter maps were analyzed manually using PlotHRM software (Lukasz Wiklendt, Flinders University), written in MATLAB (MathWorks) and JavaTM (Sun Microsystems, Santa Clara, CA). Extracellular electrical activity of colonic smooth muscle was analyzed using LabChart 8 and Spike Histogram software (ADInstruments). Action potentials and electrical oscillations within neurogenic spike bursts were discriminated to determine average firing rates using manually set thresholds and median filtering. Mechanical activities were analyzed manually using LabChart 8 software (ADInstruments).

Statistical analysis was performed by analysis of variance (1-way or 2-way), or Student 2-tailed t test for paired or unpaired data using Prism 6 (GraphPad Software, Inc, La Jolla, CA). Statistical differences were considered significant if $P < .05$. All data are presented as mean $\pm$ SEM unless otherwise stated. Lower-case "n" always indicates the number of animals.

Results

Immunohistochemistry

Immunohistochemically detectable eYFP occurred in small and large nerve cell bodies and in varicose axons throughout the colonic myenteric plexus of *CAL-ChR2*$^{Cre+}$ mice, but not littermate controls (*CAL-ChR2*$^{Cre-}$; soma size: 190 $\pm$ 5 μm^2, 192 cells, n = 6). High proportions of the nerve cell bodies containing eYFP-like immunoreactivity (eYFP-LI) also contained calretinin (CAL-LI; 97% $\pm$ 3%, n = 6) and choline acetyltransferase (ChAT-LI; 79% $\pm$ 7%, n = 5), and a small proportion contained neuronal NOS (NOS-LI; 12% $\pm$ 5%, n = 7). Conversely, nerve cell bodies containing eYFP-LI comprised 98% $\pm$ 2%, 87% $\pm$ 6%, and 9% $\pm$ 4% of all nerve cell bodies containing CAL-LI, ChAT-LI, and NOS-LI, respectively (Supplementary Table 1). Representative micrographs are shown in Figure 1*A*. This suggests the ChR2-eYFP fusion gene was predominantly expressed among calretinin-expressing, cholinergic neurons.

Patch-Clamp Electrophysiology and Calcium Imaging

Light-evoked transmembrane currents were observed under voltage-clamp conditions in cultured myenteric neurons from *CAL-ChR2*$^{Cre+}$ colon but not *Cre*$^{-}$ controls (2.8 $\pm$ 0.9 pA/pF vs 0.4 $\pm$ 0.1 pA/pF, respectively, $P < .05$, independent samples t test, n = 5; Figure 2*C, D*, and *F*). Under current clamp conditions, light stimulation evoked membrane depolarization (Figure 2*E*) and action-potential discharge in neurons from *CAL-ChR2*$^{Cre+}$ colon but not *Cre*$^{-}$ controls (depolarization: 13 $\pm$ 2.2 mV vs 0.0 $\pm$ 0.0 mV, respectively, $P < .001$, independent samples t test, n = 5; Figure 2*A* and *B*). Consistent with these electrophysiological data, calcium imaging revealed light-evoked transients in myenteric neurons of *CAL-ChR2*$^{Cre+}$ but not *Cre*$^{-}$ control colon (Figure 2*G* and *H*). These data suggest myenteric neurons in *CAL-ChR2*$^{Cre+}$ mice expressed functional light-sensitive channels.

Electrophysiological and Mechanical Recordings of Colon

Intact tube preparations of the whole colon showed ongoing, propagating contractions with intervals of 3 to 4 minutes (interval: 217 $\pm$ 24 seconds, n = 7; Figure 3, Supplementary Figure 2). This activity was tetrodotoxin (TTX)-sensitive and thus deemed neurogenic (n = 2). Neurogenic contractions occurred with bursts of smooth muscle action potentials and electrical oscillations, whose characteristics were consistent with "neurogenic spike

Figure 2. Effects of blue light application light on colonic myenteric neurons expressing eYFP/ChR2. Whole-cell recording in current clamp mode revealed light application evoked depolarization and phasic action-potential discharge in myenteric neurons from *CAL-ChR2*$^{Cre+}$ (*A*), but not *Cre*$^{-}$ control mice (*B*). In voltage-clamp mode, light promptly evoked large inward currents that terminated rapidly at offset in myenteric neurons from *CAL-ChR2*$^{Cre+}$ (*C*), but not *Cre*$^{-}$ control mice (*D*). (*E*) Average light-evoked depolarization in myenteric neurons from *CAL-ChR2*$^{Cre+}$ and *Cre*$^{-}$ control mice. Depolarization magnitude was significantly greater in *CAL-ChR2*$^{Cre+}$ mice compared with neurons from control mice. (*F*) Light-evoked current density was significantly greater in colonic myenteric neurons of *CAL-ChR2*$^{Cre+}$ mice compared with control mice. Additionally, light-evoked calcium influx in myenteric neurons from *CAL-ChR2*$^{Cre+}$ (*G*), but not *Cre*$^{-}$ control mice (*H*). KCl (100 mM).

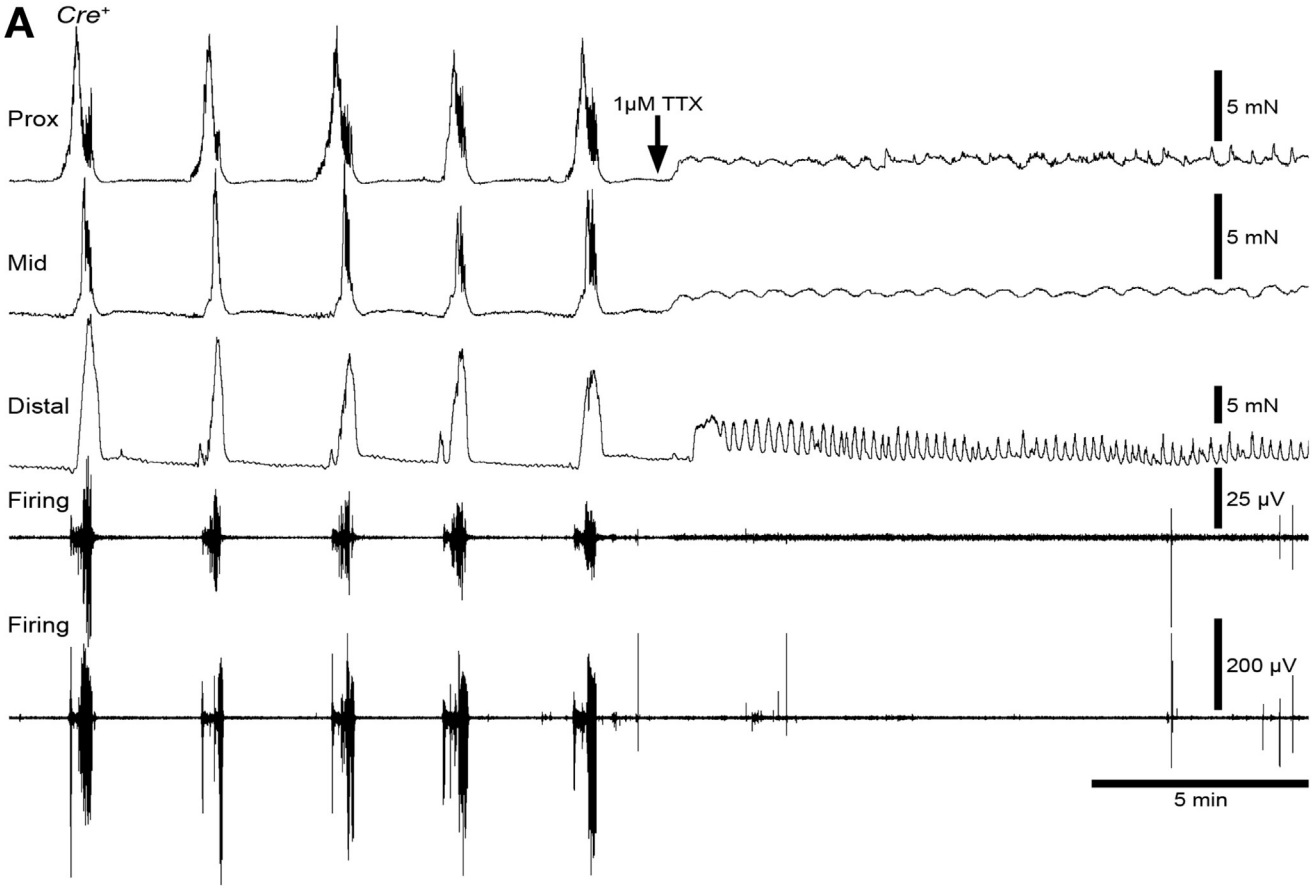
A
Cre+
Prox
1μM TTX
5 mN
Mid
5 mN
Distal
5 mN
Firing
25 μV
Firing
200 μV
5 min

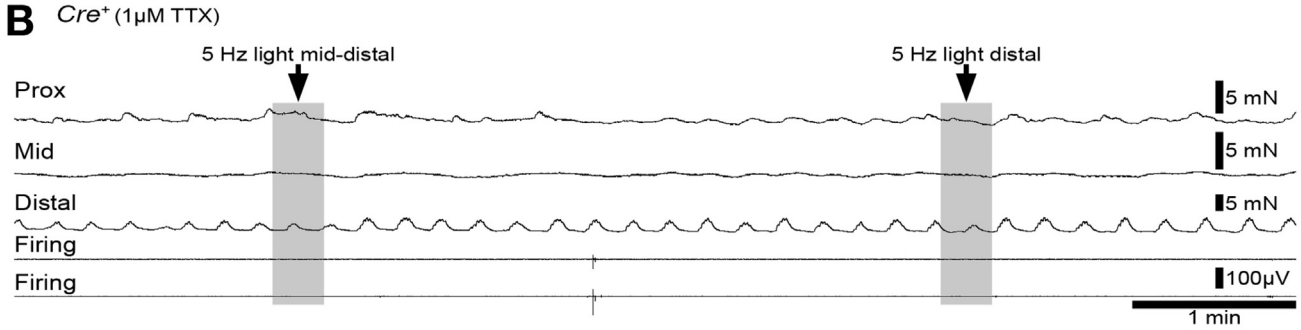
B
Cre+ (1μM TTX)
5 Hz light mid-distal
5 Hz light distal
Prox
5 mN
Mid
5 mN
Distal
5 mN
Firing
Firing
100μV
1 min

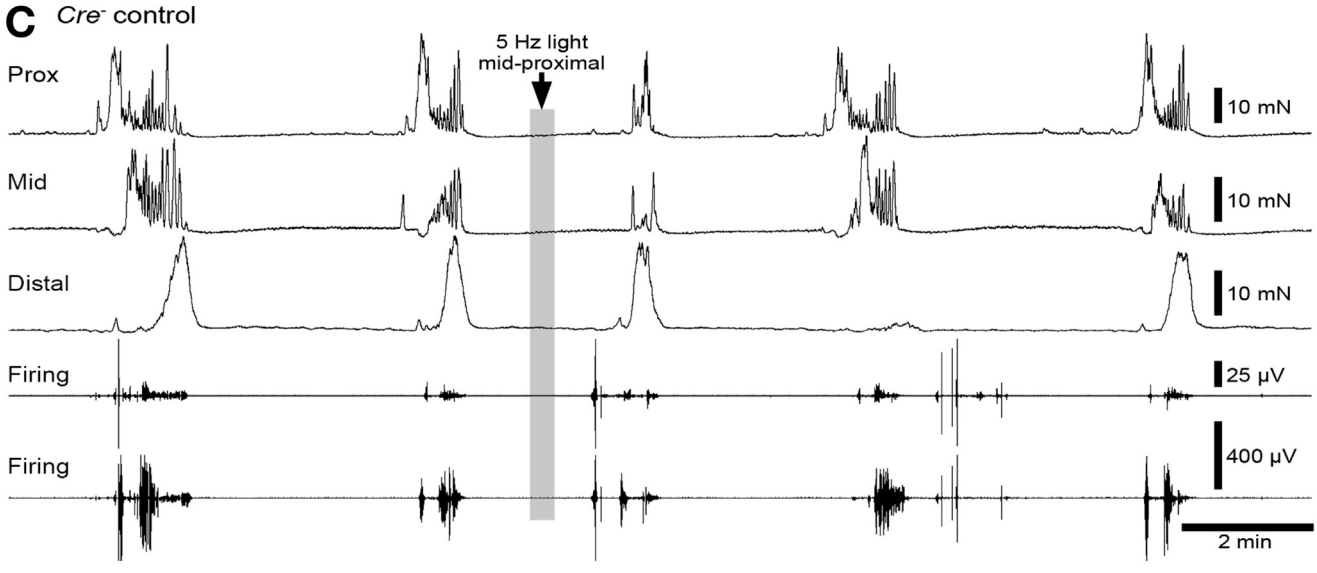
C
Cre- control
5 Hz light
mid-proximal
Prox
10 mN
Mid
10 mN
Distal
10 mN
Firing
25 μV
Firing
400 μV
2 min

bursts," described previously[16] (interval: 240 ± 19 seconds, duration: 39 ± 3 seconds, mean firing rate: 2.0 ± 0.04 Hz, n = 7; Supplementary Table 2; Figure 3, Supplementary Figure 2). In *CAL-ChR2^{Cre+}* colon, the most reliable and immediate effects of light stimulation were polarized motor responses characterized by proximal contraction and/or distal relaxation,[20] relative to the stimulation site (50/58 stimulations, n = 7; Figure 4). Polarized motor responses always occurred during the stimulation period, with short latency (mean latency from stimulus onset: 3.4 ± 0.3 seconds) and the changes in tension caused by contractions was significantly larger than those caused by relaxations (contraction amplitude 0.57 ± 0.10*g*, relaxation amplitude 0.08 ± 0.01*g*, $P < .01$, paired samples *t* test, n = 7). The effectiveness of light application in evoking polarized motor reflexes was not statistically different between the tested locations (proximal: 13/16, mid-proximal: 13/13, mid-distal: 16/17, distal: 8/12, $P = .067$, $\chi^2 = 7.2$, df = 3, n = 7). In 39 of 58 stimulations (n = 7), "premature" neurogenic contractions and spike bursts occurred after the polarized motor response (36/39 preceded by detectable polarized reflexes). Thirty-five of 39 prematurely evoked contractions propagated in a regular anterograde direction (proximal to distal), regardless of the stimulus location ($\chi^2 = 5.388$, df = 6, $P = .495$; n = 7). These neurogenic contractions occurred with a latency to peak amplitude of 34 ± 2 seconds from the onset of stimulation (Figure 4*A*, Figure 5). The contractions were deemed "premature" because their preceding interval was outside, and shorter than, the 95% confidence range of intervals of ongoing, spontaneous contractions in the same preparation (Figure 5*B*). Stimulations were intentionally timed to evoke contractions that were premature (~30–60 seconds following a spontaneous contraction). Thus, the intervals preceding the light-evoked neurogenic contractions and spike bursts were significantly reduced compared with regular spontaneous contraction intervals in *CAL-ChR2^{Cre+}* colon ($P < .05$, Bonferroni posttest, 2-way analysis of variance, *Cre*$^+$ n = 7, *Cre*$^-$ n = 4; Figure 5*C*, Supplementary Figure 3, Supplementary Table 2). However, the mechanical and electrophysiological characteristics of light-evoked propagating contractions were not otherwise significantly different from regular spontaneous contractions (Figure 5*C*, Supplementary Figure 3, Supplementary Table 2). Additionally, no significant effects of stimulation on neurogenic contraction intervals or other mechanical and electrophysiological characteristics were observed in control preparations (Supplementary Figure 3), nor were propagating contractions evoked by light stimulation in TTX (10^{-6} M; 11 stimulations, n = 2; Figure 3*B*). As with polarized reflexes, the effectiveness of light application in evoking premature neurogenic contractions was not statistically significantly different between the tested locations (proximal: 9/16, mid-proximal: 10/13, mid-distal: 13/17, distal: 7/12, $P = .900$, $\chi^2 = 0.586$, df = 3, n = 7). Light stimulations (5 Hz, 20-ms pulse width, 20-second train duration) applied in additional experiments revealed that stimulation efficacy was graded with light power density (1–40 mW/mm^2; n = 3; Supplementary Figure 4). Stimulations at light power densities above 18.5 mW/mm^2 were most reliable, evoking neurogenic contractions in more than half of stimulations applied (see Supplementary Figure 4*B* and *C*). Local motor reflexes assessed in a single preparation could be evoked by brief stimulations at light power densities as low as 2.75 mW/mm^2 (5Hz, 20-ms pulse width, 5-seconds train duration; Supplementary Figure 4*D*). Taken together, these data suggest that activation of calretinin neurons can evoke polarized motor reflexes and premature propagating neurogenic contractions, with similar efficacy along the length of the colon.

Stimulation of Colonic Motility In Vitro

Isolated mouse colons were set up in an organ bath with natural content intact. Colonic preparations initially contained an average of 4 natural pellets on removal from the animal (*CAL-ChR2^{Cre+}*: 3.8 ± 0.7, *Cre*$^-$ control: 4.4 ± 0.4, $P = .377$, independent samples *t* test, n = 5 and n = 9, respectively). Stimulations were applied at a pre-set interval of 3 minutes. After 15 minutes of light stimulation of the mid-proximal colon, 3 of 5 *CAL-ChR2^{Cre+}* preparations cleared all pellets, compared with 0 of 9 *Cre*$^-$ control preparations. On average, *CAL-ChR2^{Cre+}* preparations had expelled 75% ± 17% of starting pellets, compared with 32% ± 8% in *Cre*$^-$ controls ($P < .05$, independent samples *t* test, *Cre*$^+$ n = 5, *Cre*$^-$ n = 9; Figure 7*B*). At 30 minutes, the difference in output was not statistically significant, possibly because most *CAL-ChR2^{Cre+}* preparations lacked content after 15 minutes (75% ± 17% and 37% ± 11% of pellets, *Cre*$^+$ and *Cre*$^-$ control, respectively, $P = .056$, independent samples *t* test, *Cre*$^+$ n = 5, *Cre*$^-$ n = 9).

In addition to pellet output, neurogenic contractions were observed by video-imaging colonic wall movements (Figure 6*A* and 6*B*). Figure 6*C* shows an example of a light-evoked propagating contraction that resulted in near-complete expulsion of fecal content. Most neurogenic contractions propagated along the colon in a proximal to distal direction (*CAL-ChR2^{Cre+}*: 38/39 contractions, n = 5, *Cre*$^-$ control: 32/32 contractions, n = 9). Significantly more propagating neurogenic contractions occurred *CAL-ChR2^{Cre+}* preparations compared with *Cre*$^-$ controls, when the identical light-stimulus regimen was delivered to both *CAL-ChR2^{Cre+}* and *Cre*$^-$ control mice (7.8 ± 0.7 vs 3.8 ± 0.9,

Figure 3. Cyclic neurogenic contractions and neurogenic spike bursts. (*A*) Neurogenic contractions and neurogenic spike bursts occurred at regular intervals of approximately 2 to 3 minutes. Neurogenic spike bursts comprised regular electrical oscillations and action potentials that occurred at a frequency of approximately 2 Hz (see also Supplementary Figure 2). TTX (1 μM) promptly abolished ongoing neurogenic contractions and neurogenic spike bursts, confirming these activities were neurogenic (n = 2). TTX increased baseline tension, consistent with a tonic inhibitory effect of enteric neurons on smooth muscle. Phasic myogenic contractions can be seen in the presence of TTX. (*B*) Light stimulation applied to the *CAL-ChR2^{Cre+}* colon in the presence of TTX did not affect ongoing activity. (*C*) Light stimulation of *Cre*− control colon showed no detectable effect on ongoing neurogenic contractions.

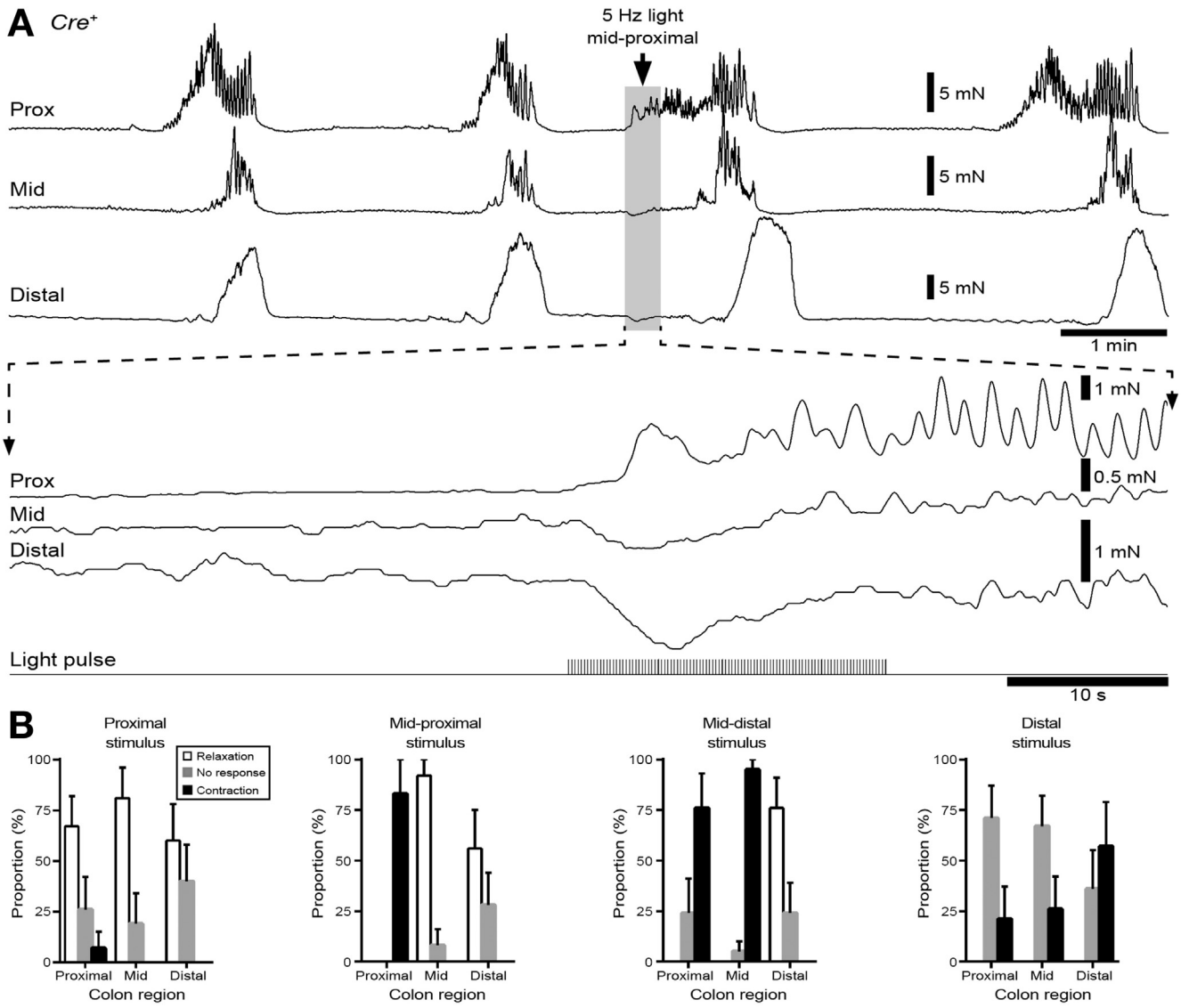

Figure 4. Light-evoked, polarized reflexes in *CAL-ChR2*$^{Cre+}$ colon. (*A*) The first mechanically detectable effects of light stimulation of the *CAL-ChR2*$^{Cre+}$ colon was contraction proximal to the site of light application and relaxation distal to the illumination site. This polarized reflex always occurred before light-evoked propagating neurogenic contraction. In this example, stimulation of the mid-proximal region evoked contraction of the proximal colon and relaxations in the middle and distal colon. (*B*) Summary of polarized reflexes, evoked by light stimulation at the proximal, mid-proximal, mid-distal, and distal region of the *CAL-ChR2*$^{Cre+}$ colon. The y axes represent the proportion of each type of motor response (relaxation, contraction, or no detectable response) in each region of colon that was evoked by the stimulus noted above the graph. In each case, the effect of stimulation was consistent with ascending excitation and descending inhibition of smooth muscle.

respectively, $P = .007$, independent samples t test; Figure 7*A*). Examples of light stimuli applied to *CAL-ChR2*$^{Cre+}$ preparations and *Cre*$^{-}$ controls are also shown in Supplementary Video 1 and 2. When the temporal and spatial characteristics of light-evoked contractions were analyzed, it was found that propagating contractions in *CAL-ChR2*$^{Cre+}$ preparations were more closely associated with light stimulation, compared with those in *Cre*$^{-}$ control preparations. On average, propagating contractions in *CAL-ChR2*$^{Cre+}$ preparations were initiated 29 ± 5 seconds from the onset of a 20-second stimulus, compared with 60 ± 7 seconds in *Cre*$^{-}$ controls ($P < .005$, independent samples t test, *Cre*$^{+}$: 39 contractions, n = 5, *Cre*$^{-}$ control: 32 contractions, n = 9; Figure 7*C*). The time difference between onset of contractions in *CAL-ChR2*$^{Cre+}$ colons and stimulation onset was also smaller when compared with intervals between randomly generated times within the recording period and their nearest stimulus (10 random times per preparation; 28 ± 4 vs 53 ± 5 seconds, *CAL-ChR2*$^{Cre+}$ and random times, respectively, $P < .005$, independent samples t test, n = 5). This was not the case in *Cre*$^{-}$ controls (10 random times per preparation; 60 ± 7 vs 63 ± 4 seconds, propagating contractions and random times, respectively, $P = .723$, independent samples t test, n = 9). Thus, contractions in *CAL-ChR2*$^{Cre+}$ but not *Cre*$^{-}$ control colon were temporally closer to stimulations than would be predicted

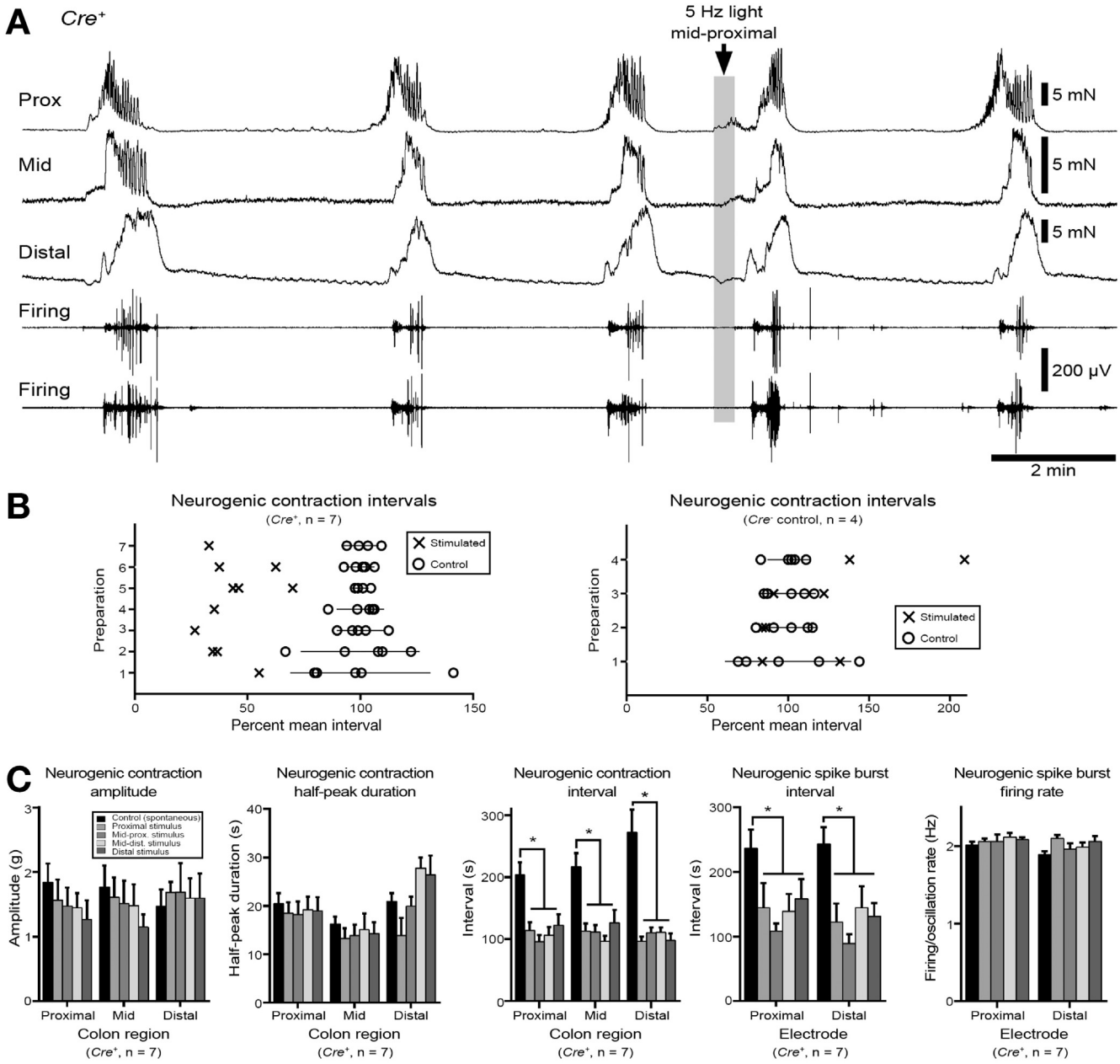

Figure 5. Effect of focal light application on neurogenic contractile and electrical activity in *CAL-ChR2*$^{Cre+}$ colon. (*A*) Example of a premature neurogenic contraction and neurogenic spike bursts evoked by light application. Note the interval between the third and fourth neurogenic contractions, which included light stimulation, was shorter than the other intervals seen between ongoing, spontaneous neurogenic contractions that lacked light stimulation. (*B*) The right graph shows examples of premature neurogenic contraction intervals evoked by mid-distal light application in 7 preparations (crosses), compared with spontaneous neurogenic contraction intervals in the same preparations (open circles; 95% confidence intervals are shown as horizontal lines). Premature neurogenic contraction intervals were shorter than *Cre*$^{-}$ control intervals and outside the 95% confidence range for spontaneous contraction intervals. For comparison, intervals containing mid-distal stimulations in *Cre*$^{-}$ control colon preparations are shown on the right (n = 4). (*C*) Summary of the effect of light stimulation on the characteristics of neurogenic contractions and spike bursts in *CAL-ChR2*$^{Cre+}$ colon. Light-evoked neurogenic contractions and spike bursts were preceded by significantly shorter intervals compared with normal ongoing neurogenic contractions ($P < .05$, Bonferroni posttest, 2-way analysis of variance, *Cre*$^{+}$ n = 7, *Cre*$^{-}$ n = 4).

by chance. Spatially, the contractions in *CAL-ChR2*$^{Cre+}$ preparations were initiated closer along the length of the gut to the location of the light stimulus than in *Cre*$^{-}$ control preparations (9 ± 1 mm vs 16 ± 1 mm in *Cre*$^{-}$ control, $P = .001$, independent samples t test, n = 5 and n = 9, respectively; Figure 7*D*). Taken together, these data suggest that light stimulation evoked neurogenic contractions and increased colonic motility, in vitro.

Stimulation of Colonic Motility In Vivo

CAL-ChR2^{Cre+} and *Cre*$^{-}$ control mice were implanted with wireless LEDs positioned opposing the proximal

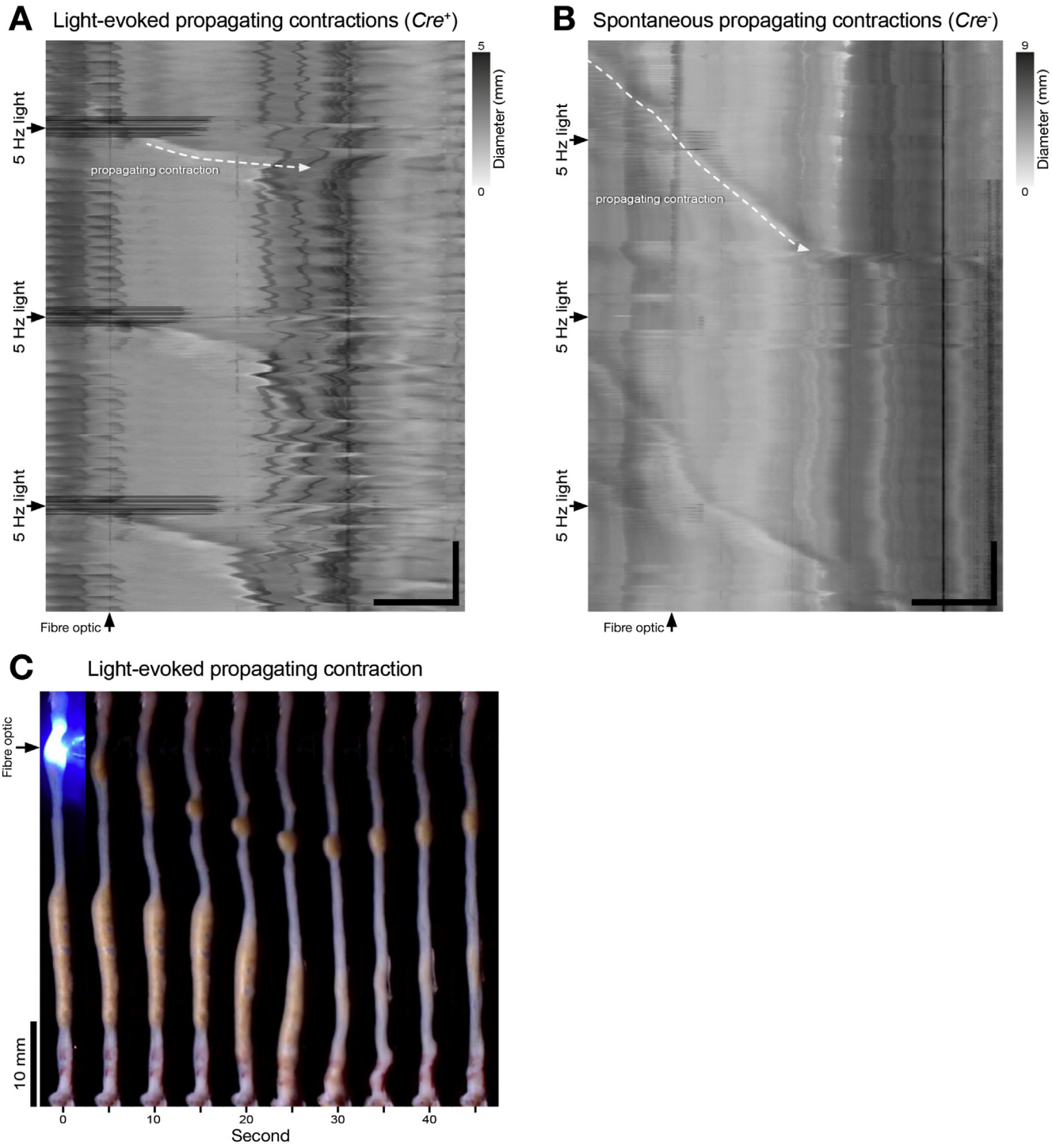

Figure 6. Examples of light stimulation of colonic motility in vitro. Representative diameter maps of light stimulation and propagating contractions in *CAL-ChR2*$^{Cre+}$ and *Cre*$^{-}$ control mice. In both examples, the oral and aboral ends of the gut are orientated left to right. Time moves forward from top to bottom. Lighter areas are more contracted, darker areas are more distended/relaxed. (*A*) Three successive propagating contractions evoked by light stimulation in *CAL-ChR2*$^{Cre+}$ colon. These propagating contractions can be seen arising from points in space and time close to the light stimulation. The first evoked contraction is marked by a dashed line. Note the location of the fiberoptic; contractions originated close to this location. Note also the higher frequency of contractions in (*A*) compared with (*B*). Dark vertical lines are artifacts caused by light pulses. Horizontal calibration, 1 minute. Vertical calibration 10 mm. (*B*) Spontaneous propagating contractions in control colon. The first contraction is also marked by a dashed line. Here, light stimulation was not temporally associated with the onset of propagating contractions. Artifacts caused by light pulses were less pronounced in this map. Horizontal calibration, 1 minute. Vertical calibration 10 mm. The effects of light stimulation on natural pellet expulsion and propagating contractions, in vitro, are summarized in graphs. (*C*) Individual video frames showing an example of light-evoked propulsive motility. Here, light stimuli applied at the proximal end of the colon evoked strong propagating contraction that caused expulsion of a large bolus of natural content.

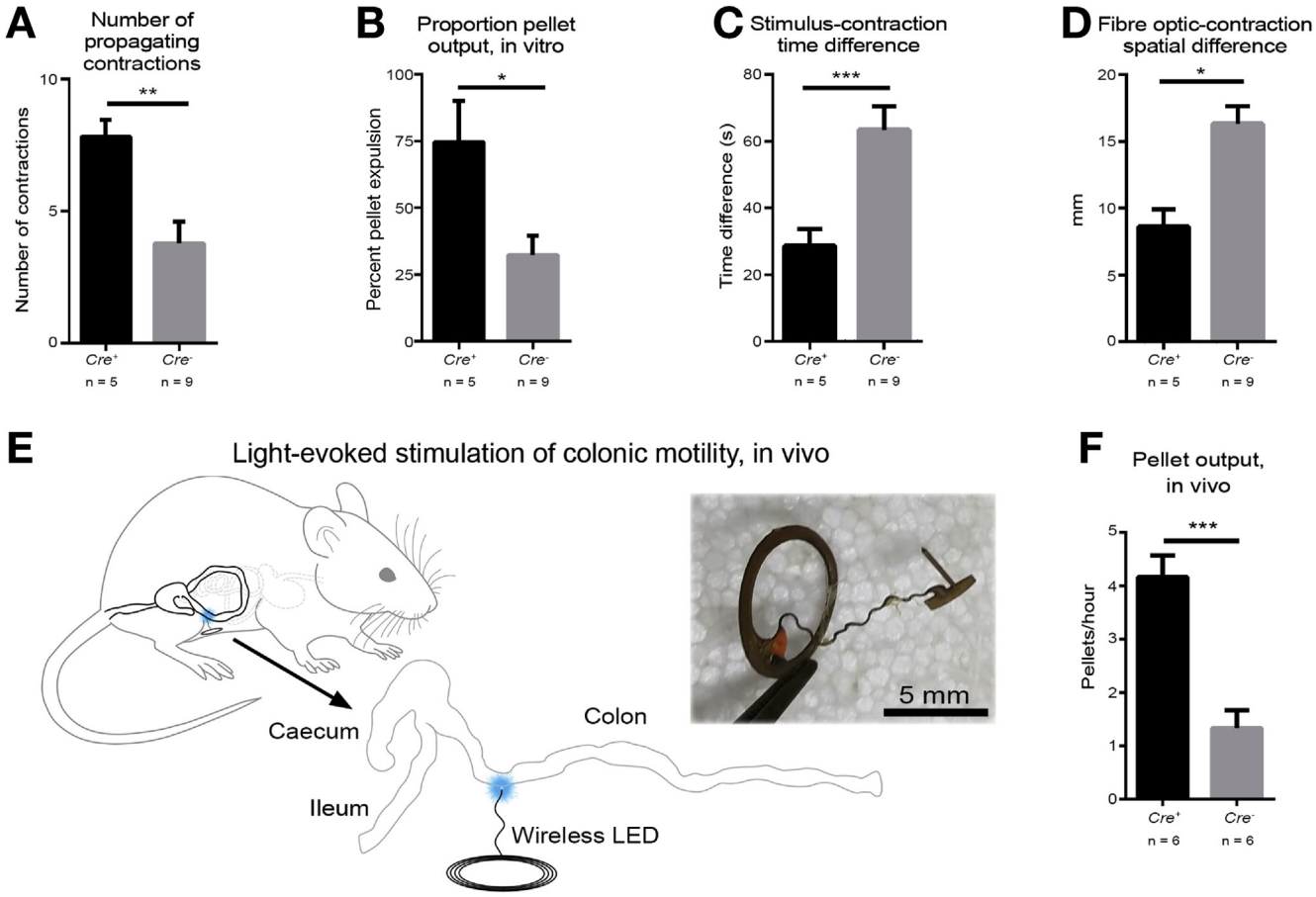

Figure 7. Light stimulation of colonic motility in vitro and in vivo. (*A*) Significantly more contractions were observed in *CAL-ChR2*$^{Cre+}$ colon over 30 minutes compared with *Cre*$^{-}$ control colon ($P = .006$, independent samples *t* test, Cre^{+} n = 5, *Cre*$^{-}$ control n = 9). (*B*) The average proportion of natural pellets expelled in 15 minutes from *CAL-ChR2*$^{Cre+}$ colons was 75% ± 17%, compared with 32% ± 8% in *Cre*$^{-}$ controls ($P < .05$, independent samples *t* test, *Cre*$^{+}$ n = 5, *Cre*$^{-}$ n = 9). (*C*) Propagating contractions in *CAL-ChR2*$^{Cre+}$ mice were initiated significantly closer in time to the onset of the light stimulus, compared with controls ($P < .001$, independent samples *t* test, *Cre*$^{+}$ n = 5, *Cre*$^{-}$ control n = 9). (*D*) Propagating contractions in *CAL-ChR2*$^{Cre+}$ colon were initiated significantly closer to the location of the fiberoptic than in *Cre*$^{-}$ controls ($P < .001$, independent samples *t* test, Cre^{+} n = 5, *Cre*$^{-}$ n = 9). (*E*) Schematic diagram showing the placement of the LED relative to the proximal colon, in vivo. The induction coil was located in parallel to the peritoneum and the LED was positioned just distal to the ceco-colonic junction, apposing the proximal colon. (*F*) Stimulation of the colon significantly increased pellet output in *CAL-ChR2*$^{Cre+}$ mice, compared with *Cre*$^{-}$ controls (4.2 ± 0.4 vs 1.3 ± 0 .3 pellets.hour^{-1}, respectively, $P < .001$, paired samples *t* test, n = 6).

colon wall, just distal to the ceco-colonic junction (Figure 7*E*). Following a week of recovery, mice were placed into recording chambers for a 1-hour acclimation, followed by 1 hour of light stimulation. Pellet output was elevated in the first hour, which is a well-characterized effect of exposure to a novel environment.[21,22] Importantly, there was no significant difference in pellet output between genotypes (*CAL-ChR2*$^{Cre+}$ and *Cre*$^{-}$ control mice: 7.3 ± 1.8 pellets vs 8.2 ± 1.7, respectively, $P = .669$, paired samples *t* test, n = 6). Pellet output was reduced in the second hour. However, pellet output was significantly increased by light stimulation of the proximal colon in *CAL-ChR2*$^{Cre+}$ mice, compared with *Cre*$^{-}$ control mice (4.2 ± 0.4 vs 1.3 ± 0.3 pellets, $P < .001$, paired samples *t* test, n = 6; Figure 7*F*). These data suggest colonic motility is increased by activation of calretinin-expressing neurons in murine proximal colon, in vivo.

Discussion

The current study is the first demonstration that optogenetic control of activity in the ENS can modify gut motility and transit of natural ingested content in vitro and in conscious mice in vivo. Focal optogenetic activation of enteric neurons can not only evoke local polarized motor reflexes, but also anterogradely propagating neurogenic contractions along the whole colon, leading to major physiological changes in fecal pellet output. This is particularly exciting because of the translational potential to improve gut motility without pharmacological agonists that act on receptors distributed in other organs or in central pathways.

Motor Behaviors Evoked by Calretinin Neurons

It has long been known that local activation of the ENS mediates stereotypical polarized motor responses

characterized by oral (proximal) contraction and aboral (distal) relaxation in response to focal mechanical or chemical stimuli.[1,2] Bayliss and Starling[23] proposed that intestinal propulsion is due to focal activation of polarized enteric neural pathways leading to oral contraction and aboral relaxation. The focal activation of calretinin neurons in the present study reliably evoked motor responses that mimicked this classic behavior. When blue light was delivered to proximal colon, primarily aboral relaxation responses occurred. However, light delivered to the distal colon primarily evoked ascending excitatory responses. Stimulation of the mid-colon evoked a combination of ascending excitatory and descending inhibitory responses. This suggests a role(s) for calretinin neurons in the enteric neural circuits that underlie polarized reflexes. Contractions on the oral side of the light stimulus were of significantly greater amplitude than relaxations evoked on the anal side. This may be explained by the preponderance of cholinergic excitatory motor neurons among calretinin-expressing neurons.[5]

The second major pattern of motor activity evoked by stimulation of calretinin neurons was propagating neurogenic contractions. This behavior has variously been referred to as "colonic migrating motor complexes,"[24] "peristalsis,"[25] and "peristaltic contractions,"[26] among others, and is the predominant form of motor behavior in murine colon. The generation of neurogenic contractions in mouse colon involves many thousands of myenteric neurons, whereby the firing activities of large populations of interneurons converge to become temporally synchronized.[27] Interestingly, evoked propagating contractions in the present study occurred approximately 30 seconds after the onset of stimulation and typically followed an initial polarized motor response. Thus, it is possible that neurogenic contractions were secondarily evoked by polarized motor responses.

The threshold number of activated neurons required to evoke neurogenic contractions is of interest. Most estimates of myenteric neuron density in mouse colon range from 270 to 600 neurons per square millimeter,[28–31] with calretinin neurons comprising approximately 35%.[4] Given that the area of direct illumination in the present study ranged from 0.0594 to 0.0987 mm^2, this suggests that on average 6 to 21 myenteric calretinin nerve cell bodies were directly illuminated, in addition to their axons, axons of passage, and varicosities. It is possible that more neurons were recruited by photon scattering, but the degree to which this contributed in the present study is unclear. The observation that induction of neurogenic contractions occurred at a higher threshold light density than polarized motor reflexes, supports this possibility and that higher numbers of calretinin neurons may be required to initiate neurogenic contractions compared with polarized reflexes. In addition, calretinin neurons occur in the colonic submucous plexus,[4,32,33] and are active during neurogenic contractions.[34] Higher light power densities may more readily penetrate through to these cells. The possibility that calretinin submucous neurons were activated in the present study and contributed to generation of neurogenic contractions cannot be ruled out.

Electrical Vs Optogenetic Stimulation of Colon

Transmural electrical stimulation can also evoke premature neurogenic propagating contractions,[35] and neurogenic spike bursts in the murine colon, in vitro.[16] However, specific activation of calretinin neurons in the present study produced some qualitatively different effects compared with electrical stimulation that may be of therapeutic relevance. For example, electrical stimulation evokes premature neurogenic contractions that propagates both orally and anally along the gut from the point of stimulation, thereby producing anterograde activity distal to the stimulus and retrograde activity proximally.[35] This effect can have undesired consequences where electrical stimulation of the gut has been tested in vivo,[36] leading to approaches that use sequential activation of multiple implanted electrodes along the gut to force anterograde activity.[37] In contrast, the evoked propagating contractions in the present study were predominantly anterograde, regardless of the stimulation location. This may represent an advantage over electrical stimulation. In addition, the efficacy of electrical stimulation may be location-dependent.[35] Electrical nerve stimulation of the proximal colon was ineffective, whereas distal colonic stimulation was most efficacious, evoking neurogenic contraction in approximately 66% of trials (similar to the overall efficacy of 63% in the present study). Unlike electrical stimulation, optogenetic stimulation of calretinin neurons in the present study showed a similar efficacy in evoking propagating neurogenic contractions from locations along the entire length of the colon. Calretinin-expressing neurons are predominantly excitatory cholinergic neurons in the ENS.[4,5,38,39] It is therefore possible that biased activation of excitatory enteric neurons in the present study may underlie this difference, or that electrical stimulation may limit ENS excitability distal to the site of stimulation by recruiting large numbers of descending inhibitory neurons (in addition to ascending excitatory neurons).

To date, localized effects on smooth muscle electrical behavior has been demonstrated in studies using optogenetic control of enteric neurons.[40,41] Rakhilin et al.[41] demonstrated ChR2-mediated activation of nitrergic inhibitory enteric neurons causes localized inhibition of smooth muscle action potentials in the small intestine. Stamp et al.[40] have shown that transplanted neural stem cells expressing ChR2 were functionally integrated into enteric neural circuits, generating local excitatory and inhibitory junction potentials in smooth muscle, as well as synaptic inputs to other enteric neurons in response to light stimuli. We report that in the whole intact colon, the focal stimulation of colonic myenteric calretinin-expressing neurons is sufficient to evoke local motor reflexes, neurogenic propagating contractions, and significant increases in fecal pellet output.

Conclusion

We provide the first demonstration that the excitability of the ENS and colonic motility can be controlled by optogenetics. The findings reveal that brief pulses of blue light to the colon of $CAL\text{-}ChR2^{Cre+}$ mice are sufficient to evoke a

premature neurogenic contraction that directly leads to a significant increase in fecal pellet output both in freely moving, conscious mice and in isolation, in vitro. This new approach could prove very effective in improving gastrointestinal transit in mammals that have impaired transit (eg, constipation) without conventional agonists that commonly stimulate not only the ENS, but also have off-target side effects in other organ systems.

Supplementary Material

Note: To access the supplementary material accompanying this article, visit the online version of *Gastroenterology* at www.gastrojournal.org, and at https://doi.org/10.1053/j.gastro.2018.05.029.

References

1. Furness JB. The enteric nervous system. Carlton, Victoria: Blackwell Publishing, 2006.
2. Wood JD. Integrative functions of the enteric nervous system. In: Johnson LR, ed. Physiology of the gastrointestinal tract. Volume 1. 5th ed. San Diego, CA: Elsevier, 2012.
3. Bayliss WM, Starling EH. The movements and the innervation of the large intestine. J Physiol 1900;26:11.
4. Sang Q, Young HM. Chemical coding of neurons in the myenteric plexus and external muscle of the small and large intestine of the mouse. Cell Tissue Res 1996; 284:39–53.
5. Sang Q, Young HM. The identification and chemical coding of cholinergic neurons in the small and large intestine of the mouse. Anat Rec 1998;251:185–199.
6. Wood JD, Brann LR, Vermillion DL. Electrical and contractile behavior of large intestinal musculature of piebald mouse model for Hirschsprung's disease. Dig Dis Sci 1986;31:638–650.
7. Kunze WAA, Furness JB. The enteric nervous system and regulation of intestinal motility. Annu Rev Physiol 1999;61:117–142.
8. Feng J, Hibberd TJ, Luo J, et al. Optogenetic induction of propagating colonic motor complexes and silencing of colonic motility using Cre-inducible activation and inactivation of calretinin-expressing neurons. Gastroenterology 2017;152:S102.
9. Madisen L, Mao T, Koch H, et al. A toolbox of Cre-dependent optogenetic transgenic mice for light-induced activation and silencing. Nat Neurosci 2012; 15:793–802.
10. Hanks JH, Wallace RE. Relation of oxygen and temperature in the preservation of tissues by refrigeration. Exp Biol Med (Maywood) 1949;71:196–200.
11. Smith TH, Ngwainmbi J, Grider JR, et al. An in-vitro preparation of isolated enteric neurons and glia from the myenteric plexus of the adult mouse. J Vis Exp 2013; 78:e50688–e50688.
12. Feng J, Luo J, Mack MR, et al. The antimicrobial peptide human beta-defensin 2 promotes itch through Toll-like receptor 4 signaling in mice. J Allergy Clin Immunol 2017;140:885–888.e6.
13. Feng J, Luo J, Yang P, et al. Piezo2 channel-Merkel cell signaling modulates the conversion of touch to itch. Science 2018;360:530–533.
14. **Liu S, Feng J**, Luo J, et al. Eact, a small molecule activator of TMEM16A, activates TRPV1 and elicits pain- and itch-related behaviours. Br J Pharmacol 2016; 173:1208–1218.
15. **Feng J, Yang P**, Mack MR, et al. Sensory TRP channels contribute differentially to skin inflammation and persistent itch. Nat Commun 2017;8:980.
16. Hibberd TJ, Costa M, Travis L, et al. Neurogenic and myogenic patterns of electrical activity in isolated intact mouse colon. Neurogastroenterol Motil 2017; 29:e13089.
17. Barnes KJ, Beckett EA, Brookes SJH, et al. Control of intrinsic pacemaker frequency and velocity of colonic migrating motor complexes in mouse. Front Neurosci 2014;8:96.
18. Hennig GW, Costa M, Chen BN, et al. Quantitative analysis of peristalsis in the guinea-pig small intestine using spatio-temporal maps. J Physiol 1999;517: 575–590.
19. **Shin G, Gomez AM, Al-Hasani R**, et al. Flexible near-field wireless optoelectronics as subdermal implants for broad applications in optogenetics. Neuron 2017; 93:509–521.
20. Grider JR. Neurotransmitters mediating the intestinal peristaltic reflex in the mouse. Journal of Pharmacology and Experimental Therapeutics 2003;307:460–467.
21. Million M, Wang L, Stenzel-Poore MP, et al. Enhanced pelvic responses to stressors in female CRF-overexpressing mice. Am J Physiol Regul Integr Comp Physiol 2007;292:R1429–R1438.
22. Wang L, Gourcerol G, Yuan PQ, et al. Peripheral peptide YY inhibits propulsive colonic motor function through Y2 receptor in conscious mice. Am J Physiol Gastrointest Liver Physiol 2010;298:G45–G56.
23. Bayliss WM, Starling EH. The movements and innervation of the small intestine. J Physiol 1899;24:44.
24. Fida R, Lyster DJ, Bywater RA, et al. Colonic migrating motor complexes (CMMCs) in the isolated mouse colon. Neurogastroenterol Motil 1997;9:99–107.
25. Gribovskaja-Rupp I, Babygirija R, Takahashi T, et al. Autonomic nerve regulation of colonic peristalsis in guinea pigs. J Neurogastroenterol Motil 2014;20:185.
26. D'Antona G, Hennig GW, Costa M, et al. Analysis of motor patterns in the isolated guinea-pig large intestine by spatio-temporal maps. Neurogastroenterol Motil 2001;13:483–492.
27. **Spencer NJ, Hibberd TJ**, Travis L, et al. Identification of a Rhythmic Firing Pattern in the Enteric Nervous System That Generates Rhythmic Electrical Activity in Smooth Muscle. J Neurosci 2018;38:5507–5522.
28. Sibaev A, Franck H, Vanderwinden J-M, et al. Structural differences in the enteric neural network in murine colon: impact on electrophysiology. Am J Physiol 2003; 285:G1325–G1334.
29. Gamage PP, Ranson RN, Patel BA, et al. Myenteric neuron numbers are maintained in aging mouse distal colon. Neurogastroenterol Motil 2013;25:e495–e505.

30. Roberts RR, Bornstein JC, Bergner AJ, et al. Disturbances of colonic motility in mouse models of Hirschsprung's disease. Am J Physiol Gastrointest Liver Physiol 2008;294:G996–G1008.
31. Beraldi EJ, Soares A, Borges SC, et al. High-fat diet promotes neuronal loss in the myenteric plexus of the large intestine in mice. Dig Dis Sci 2015;60:841–849.
32. Nasser Y, Ho W, Sharkey KA. Distribution of adrenergic receptors in the enteric nervous system of the guinea pig, mouse, and rat. J Comp Neurol 2006; 495:529–553.
33. Stewart AL, Anderson RB, Young HM. Characterization of lacZ-expressing cells in the gut of embryonic and adult DβH-nlacZ mice. J Comp Neurol 2003; 464:208–219.
34. Okamoto T, Bayguinov P, Broadhead M, et al. Ca2+ transients in submucous neurons during the colonic migrating motor complex in the isolated murine large intestine. Neurogastroenterol Motil 2012;24:769–778.
35. Spencer NJ, Bywater RA. Enteric nerve stimulation evokes a premature colonic migrating motor complex in mouse. Neurogastroenterol Motil 2002;14:657–665.
36. Kelly KA, Code CF. Duodenal-gastric reflux and slowed gastric emptying by electrical pacing of the canine duodenal pacesetter potential. Gastroenterology 1977; 72:429–433.
37. Amaris MA, Rashev PZ, Mintchev MP, et al. Microprocessor controlled movement of solid colonic content using sequential neural electrical stimulation. Gut 2002; 50:475–479.
38. Furness JB, Robbins HL, Xiao J, et al. Projections and chemistry of Dogiel type II neurons in the mouse colon. Cell Tissue Res 2004;317:1–12.
39. Sang Q, Williamson S, Young HM. Projections of chemically identified myenteric neurons of the small and large intestine of the mouse. J Anat 1997;190:209–222.
40. Stamp LA, Gwynne RM, Foong JPP, et al. Optogenetic demonstration of functional innervation of mouse colon by neurons derived from transplanted neural cells. Gastroenterology 2017; 152:1407–1418.
41. **Rakhilin N, Barth B**, Choi J, et al. Simultaneous optical and electrical in vivo analysis of the enteric nervous system. Nat Commun 2016;7:11800.

Author names in bold designate shared co-first authorship.

Received October 27, 2017. Accepted April 12, 2018.

Reprint requests
Address requests for reprints to: Nick Spencer, PhD, College of Medicine and Public Health and Centre for Neuroscience, Flinders University, GPO Box 2100, Adelaide, South Australia 5001. e-mail: nicholas.spencer@flinders.edu.au; fax: +61 8 8204 5768 or Hongzhen Hu, PhD, Department of Anesthesiology, The Center for the Study of Itch, Washington University, St Louis, Misssouri, 63110. e-mail: hongzhen.hu@wustl.edu; fax: (314) 362-8571.

Acknowledgments
We thank Lauren Keightley and Lukasz Wiklendt for assistance with spatiotemporal mapping and preparation of the manuscript, Lee Travis for testing effects of light power density on colonic motility in vitro, and SA Biomedical Engineering, Research, and Teaching Team for supporting this project through the development and construction of the equipment used.

Conflicts of interest
The authors disclose the following: Robert W. Gereau IV is a co-founder of Neurolux, a company that manufactures the wireless optoelectronic devices used for the in vivo optogenetic experiments in the present study. All remaining authors disclose no conflicts.

Funding
This work was supported by grants from the National Institutes of Health (NIH) (R01GM101218 and R01DK103901 to Hongzhen Hu), Washington University School of Medicine Digestive Disease Research Core Center (NIDDK P30 DK052574), The Center for the Study of Itch of Department of Anesthesiology at Washington University School of Medicine (to Hongzhen Hu), NIH SPARC Award (NIBIB U18EB021793) and NIH Director's Transformative Research Award (TR01 NS081707) to Robert W. Gereau IV. Timothy J. Hibberd was supported by a grant (1127140) from the National Health and Medical Research Council of Australia to Nick J. Spencer. Vijay K. Samineni was supported by the Urology Care Foundation Research Scholars Program, and the Kailash Kedia Research Scholar Award.

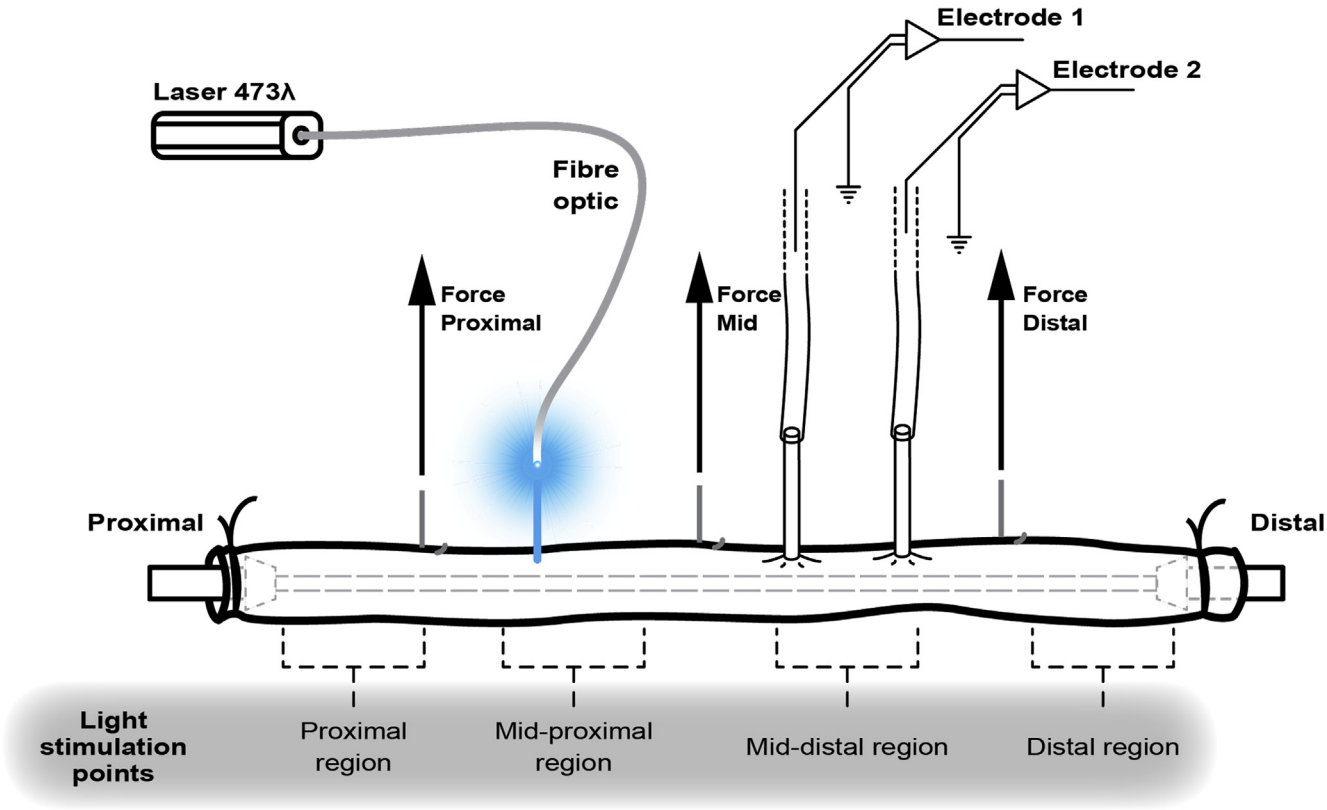

Supplementary Figure 1. Schematic diagram of the experimental setup used for mechanical and electrical recordings of neurogenic contractions and spike bursts. Light stimulation was applied at the regions indicated.

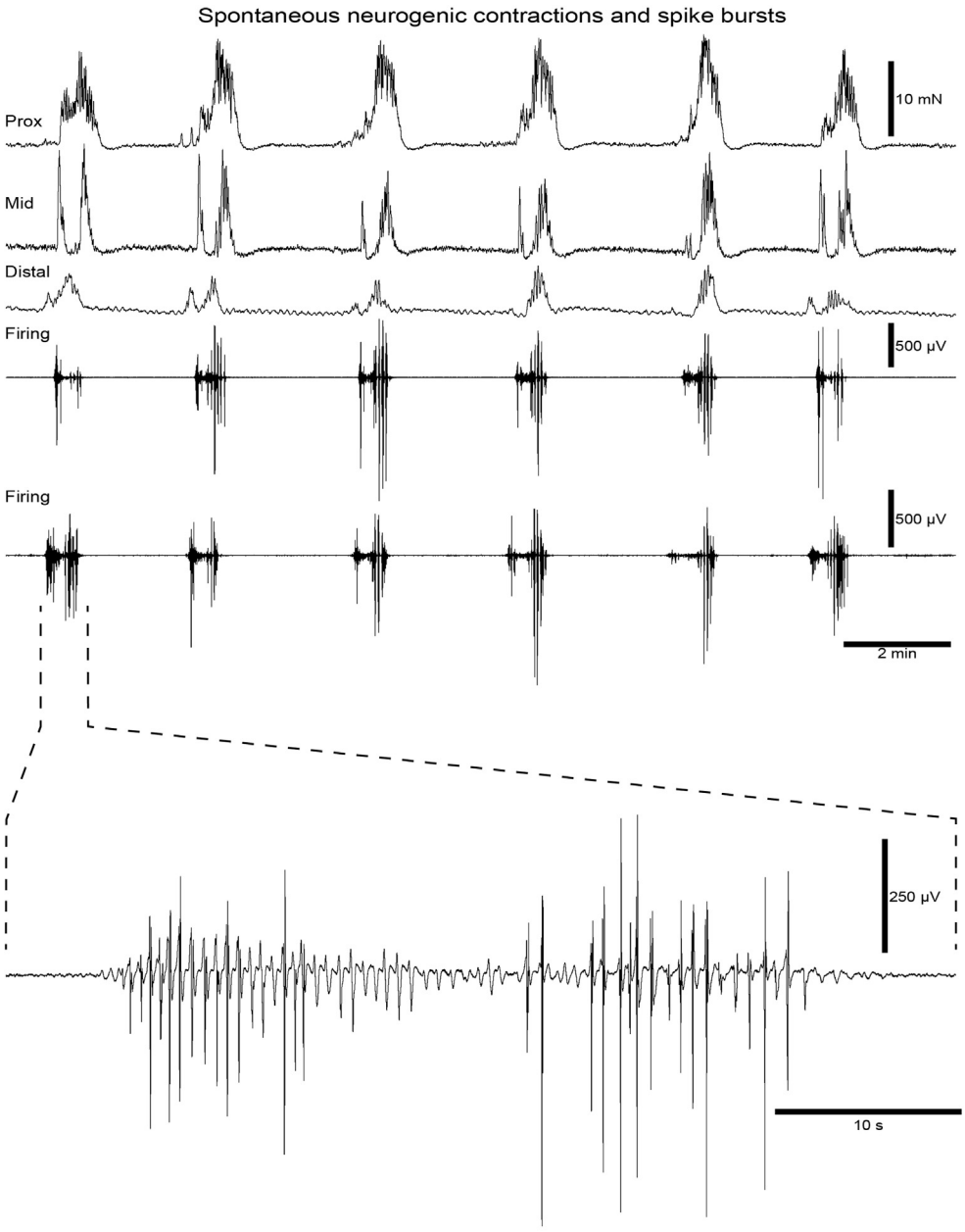

Supplementary Figure 2. Ongoing neurogenic contractions and spike bursts in *CAL-ChR2^{Cre+}* colon. Here, neurogenic contractions and spike bursts occured at regular intervals of about 2-3 minutes. Neurogenic spikes bursts were comprised of regular electrical oscillations and action potentials with a frequency of about 2Hz.

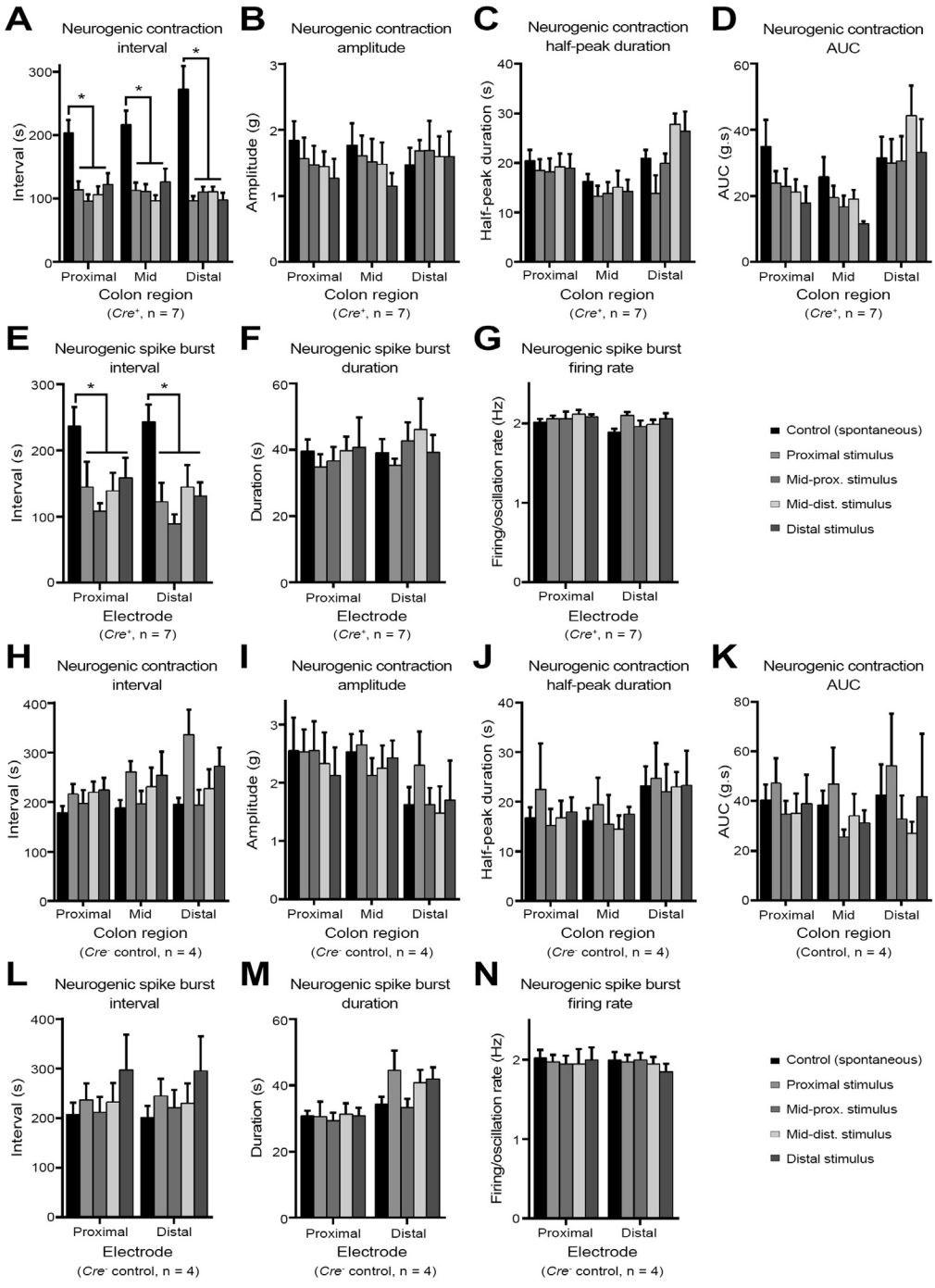

Supplementary Figure 3. Characteristics of spontaneous and evoked neurogenic contractions and spike bursts in *CAL-ChR2*$^{Cre+}$ mice (*A-G*) and Cre$^-$ controls (*H-N*). Intervals preceding neurogenic contractions and spike bursts were significantly reduced by stimulation in *CAL-ChR2*$^{Cre+}$ colon (*A* and *E*) but not in *Cre*$^-$ controls (*H* and *I*). * $P < 0.05$ Bonferroni post-test, 2-way ANOVA, *Cre*$^+$ n = 7, *Cre*$^-$ n = 4. Error bars, s.e.m.

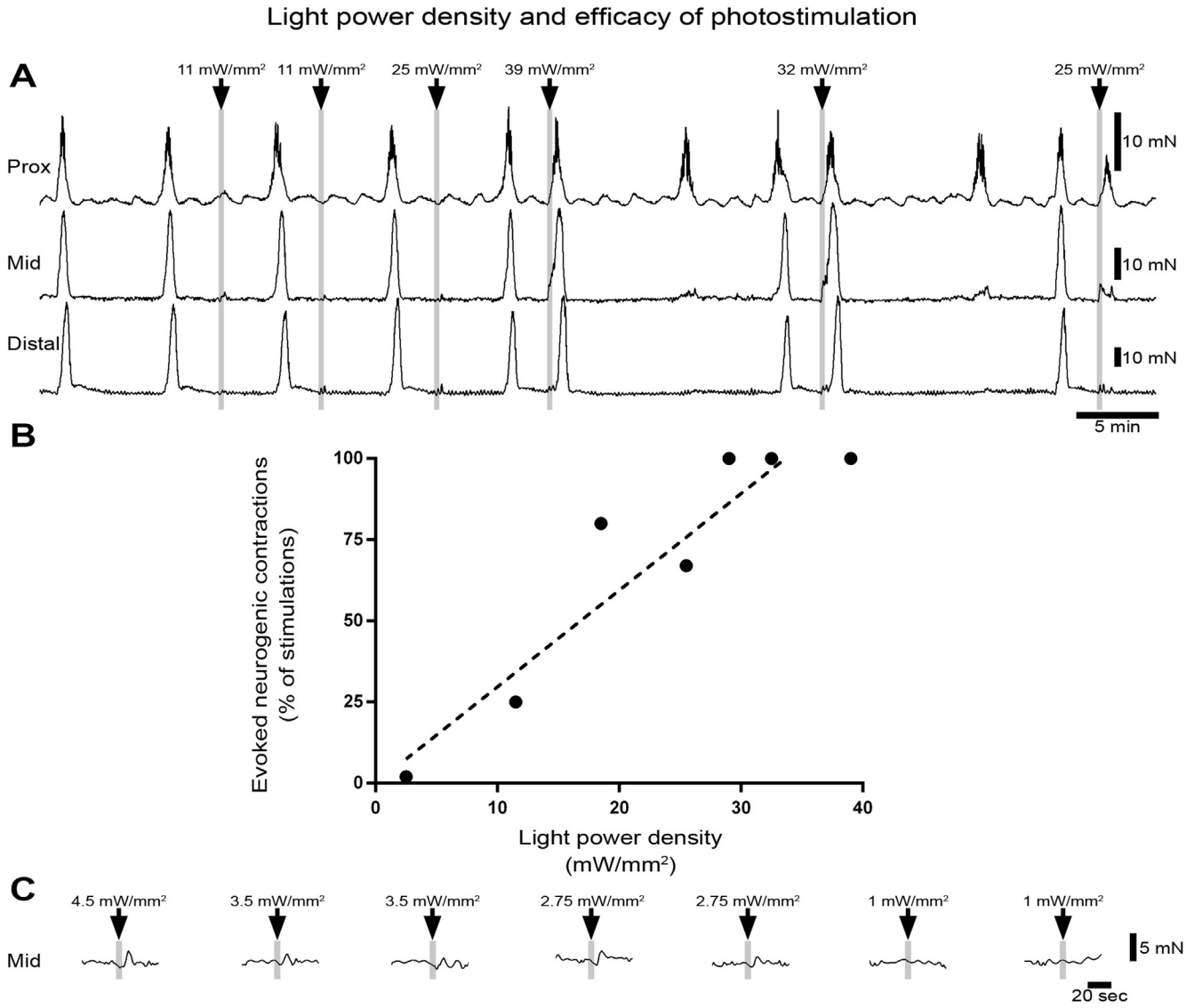

Supplementary Figure 4. Light power density and efficacy of stimulation was graded, increasing in reliabillty with increases in power density. *A* Examples of photostimulation (5 Hz, 20 ms pulse width, 20 seconds train duration) applied at different power densities to the mid-distal colon. In this preparation stimulations <25 mW/mm^2 gave attenuated neurogenic contractions or local polarized reflexes while higher power stimulation (>25 mW/mm^2) reliably evoked propagating neurogenic contractions *B* Scater plot showing light power density versus neurogenic contractions. Overall, power densities greater than 18.5 mW/mm^2 had the most reliable rates or response ($n = 3$). *C* Local motor reflexes were evoked at lower power densities. In these examples from the same preparation, small descending relaxations (followed by contraction) were detectable during photostimulation at a power density of 2.75 mW/mm^2 (mid-proximal colon, 5 Hz, 20 ms pulse width, 5 seconds train duration).

Supplementary Table 1. Immunohistochemical Characteristics of eYFP/ChR2 Neurons

	%
eYFP-LI myenteric nerve cell bodies that were CAL-LI	97 ± 7 (72 cells, n = 6)
CAL-LI myenteric nerve cell bodies that were eYFP-LI	98 ± 4 (72 cells, n = 6)
eYFP-LI myenteric nerve cell bodies that were ChAT-LI	79 ± 14 (75 cells, n = 5)
ChAT-LI myenteric nerve cell bodies that were eYFP-LI	87 ± 11 (75 cells, n = 5)
eYFP-LI myenteric nerve cell bodies that were NOS-LI	12 ± 13 (114 cells, n = 7)
NOS-LI myenteric nerve cell bodies that were eYFP-LI	9 ± 11 (114 cells, n = 7)

Supplementary Table 2. Characteristics of Spontaneous and Evoked Neurogenic Contractions and Spike Bursts

	CAL-ChR2^{Cre+}																	
	Neurogenic contraction interval (*s*)			Neurogenic contraction peak amplitude (*g*)			Neurogenic contraction AUC (*g.s*)			Neurogenic contraction half-peak duration (*s*)			Neurogenic spike burst characteristics (proximal electrode)			Neurogenic spike burst characteristics (distal electrode)		
	proximal colon	mid-colon	distal colon	proximal colon	mid-colon	distal colon	proximal colon	mid-colon	distal colon	proximal colon	mid-colon	distal colon	interval (*s*)	duration (*s*)	MFR (*Hz*)	interval (*s*)	duration (*s*)	MFR (*Hz*)
Control	204 ± 22	217 ± 24	272 ± 39	1.8 ± 0.3	1.8 ± 0.4	1.5 ± 0.3	35 ± 9	26 ± 6	32 ± 7	21 ± 3	16 ± 2	21 ± 2	237 ± 30	40 ± 4	2.0 ± 0.04	243 ± 28	39 ± 4	1.9 ± 0.05
Stim. (Prox)	114 ± 15[a]	113 ± 14	96 ± 9	1.6 ± 0.4	1.6 ± 0.3	1.7 ± 0.2	24 ± 4	19 ± 4	30 ± 8	18 ± 3	13 ± 2	14 ± 4	145 ± 43[a]	35 ± 4	2.1 ± 0.04	123 ± 33[a]	35 ± 2	2.1 ± 0.05
Stim. (Mid-Prox)	96 ± 12[a]	112 ± 12	110 ± 10	1.5 ± 0.3	1.5 ± 0.4	1.7 ± 0.5	23 ± 6	17 ± 4	31 ± 8	18 ± 3	14 ± 3	20 ± 2	108 ± 14[a]	37 ± 5	2.1 ± 0.1	89 ± 17[a]	43 ± 6	2 ± 0.08
Stim. (Mid-Dist)	107 ± 14[a]	97 ± 9	111 ± 9	1.4 ± 0.2	1.5 ± 0.4	1.6 ± 0.3	21 ± 4	19 ± 3	44 ± 10	19 ± 3	15 ± 4	28 ± 2	139 ± 30[a]	40 ± 5	2.1 ± 0.06	145 ± 36[a]	46 ± 10	2 ± 0.07
Stim. (Distal)	122 ± 19[a]	126 ± 23	98 ± 13	1.3 ± 0.3	1.1 ± 0.2	1.6 ± 0.4	18 ± 6	12 ± 1	33 ± 11	19 ± 3	14 ± 3	26 ± 4	159 ± 33[a]	41 ± 10	2.1 ± 0.03	132 ± 23[a]	39 ± 6	2.1 ± 0.08

	Cre^{-} control																	
	Neurogenic contraction interval (*s*)			Neurogenic contraction peak amplitude (*g*)			Neurogenic contraction AUC (*g.s*)			Neurogenic contraction half-peak duration (*s*)			Neurogenic spike burst characteristics (proximal electrode)			Neurogenic spike burst characteristics (distal electrode)		
	proximal colon	mid-colon	distal colon	proximal colon	mid-colon	distal colon	proximal colon	mid-colon	distal colon	proximal colon	mid-colon	distal colon	interval (*s*)	duration (*s*)	MFR (*Hz*)	interval (*s*)	duration (*s*)	MFR (*Hz*)
Control	179 ± 15	188 ± 19	196 ± 14	2.6 ± 0.6	2.5 ± 0.4	1.6 ± 0.3	40 ± 7	38 ± 7	43 ± 14	17 ± 3	16 ± 3	23 ± 5	207 ± 28	31 ± 2	2 ± 0.12	201 ± 27	34 ± 3	2 ± 0.12
Stim. (Prox)	216 ± 24	261 ± 26	336 ± 58	2.5 ± 0.5	2.7 ± 0.3	2.3 ± 0.7	47 ± 11	47 ± 17	54 ± 24	22 ± 11	19 ± 6	25 ± 8	236 ± 39	30 ± 5	2 ± 0.1	245 ± 40	44 ± 7	2 ± 0.1
Stim. (Mid-Prox)	197 ± 31	196 ± 30	194 ± 36	2.5 ± 0.6	2.1 ± 0.3	1.6 ± 0.3	35 ± 6	25 ± 3	33 ± 11	15 ± 4	15 ± 7	22 ± 6	212 ± 35	29 ± 3	2 ± 0.12	221 ± 41	33 ± 3	2 ± 0.11
Stim. (Mid-Dist)	219 ± 26	231 ± 45	227 ± 45	2.3 ± 0.6	2.2 ± 0.4	1.5 ± 0.5	35 ± 9	34 ± 10	27 ± 6	17 ± 4	14 ± 3	23 ± 4	232 ± 45	31 ± 4	2 ± 0.21	230 ± 46	41 ± 5	2 ± 0.1
Stim. (Distal)	224 ± 28	254 ± 55	273 ± 43	2.1 ± 0.6	2.4 ± 0.3	1.7 ± 0.8	39 ± 14	31 ± 6	42 ± 29	18 ± 3	17 ± 2	23 ± 8	297 ± 83	31 ± 3	2 ± 0.18	295 ± 81	42 ± 4	1.9 ± 0.12

NOTE. Values represent mean ± SEM.
AUC, area under the curve; Dist, distal; MFR, mean firing rate; Prox, proximal.
[a]$P < .05$ compared with control, Bonferroni posttest, 2-way analysis of variance.